Regulation and functional consequences of $mGlu_4$ RNA editing

CHRISTOPHER S. HOFMANN,[1,2] SHERIDAN CARRINGTON,[1,2] ANDREW N. KELLER,[3] KAREN J. GREGORY,[3] and COLLEEN M. NISWENDER[1,2,4]

[1]Department of Pharmacology, Vanderbilt University, Nashville, Tennessee 37232, USA

[2]Warren Center for Neuroscience Drug Discovery, Vanderbilt University, Nashville, Tennessee 37232, USA

[3]Department of Pharmacology and Drug Discovery Biology, Monash Institute of Pharmaceutical Sciences, Monash University, Parkville, Victoria 3052, Australia

[4]Vanderbilt Kennedy Center, Vanderbilt University Medical Center, Nashville, Tennessee 37203, USA

ABSTRACT

Metabotropic glutamate receptor 4 ($mGlu_4$) is one of eight mGlu receptors within the Class C G protein-coupled receptor superfamily. $mGlu_4$ is primarily localized to the presynaptic membrane of neurons where it functions as an auto and heteroreceptor controlling synaptic release of neurotransmitter. $mGlu_4$ is implicated in numerous disorders and is a promising drug target; however, more remains to be understood about its regulation and pharmacology. Using high-throughput sequencing, we have validated and quantified an adenosine-to-inosine (A-to-I) RNA editing event that converts glutamine 124 to arginine in $mGlu_4$; additionally, we have identified a rare but novel K129R site. Using an in vitro editing assay, we then validated the pre-mRNA duplex that allows for editing by ADAR enzymes and predicted its conservation across the mammalian species. Structural modeling of the $mGlu_4$ protein predicts the Q124R substitution to occur in the B helix of the receptor that is critical for receptor dimerization and activation. Interestingly, editing of a receptor homodimer does not disrupt G protein activation in response to the endogenous agonist, glutamate. Using an assay designed to specifically measure heterodimer populations at the surface, however, we found that Q124R substitution decreased the propensity of $mGlu_4$ to heterodimerize with $mGlu_2$ and $mGlu_7$. Our study is the first to extensively describe the extent and regulatory factors of RNA editing of $mGlu_4$ mRNA transcripts. In addition, we have proposed a novel functional consequence of this editing event that provides insights regarding its effects in vivo and expands the regulatory capacity for mGlu receptors.

Keywords: A-to-I editing; RNA; $mGlu_4$; molecular biology

INTRODUCTION

The major excitatory neurotransmitter in the mammalian central nervous system, L-glutamate, mediates its effects through two classes of receptors: ionotropic and metabotropic (Meldrum 2000). While ionotropic receptors function as ligand-gated ion channels mediating excitatory synaptic signaling, metabotropic glutamate (mGlu) receptors are class C G protein-coupled receptors that modulate neuronal plasticity, long-term potentiation (LTP), and long-term depression (LTD) through second messengers and effector proteins. This dual action of glutamate as an excitatory and modulatory neurotransmitter underlies the mechanisms for learning, memory, and synaptic plasticity (Willard and Koochekpour 2013; Reiner and Levitz 2018). The eight members of the mGlu receptor family are separated into three groups determined by their sequence homology, pharmacology, and downstream heterotrimeric G-protein coupling profile.

$mGlu_4$, a group III mGlu receptor, is expressed throughout multiple regions of the human brain including the hippocampus, hypothalamus, caudate nucleus, cortex, putamen, and cerebellum (Flor et al. 1995; Makoff et al. 1996). Similar to other group III receptors ($mGlu_4$, $mGl6_4$, $mGlu_8$, $mGlu_8$), $mGlu_4$ is predominantly expressed presynaptically and signals primarily through $G_{i/o}$ to inhibit neurotransmitter release, an effect which is inhibitory at glutamatergic presynaptic terminals and excitatory at GABAergic presynaptic terminals (Semyanov and Kullmann 2000; Lorez et al.

Corresponding author: colleen.niswender@vanderbilt.edu

Article is online at http://www.rnajournal.org/cgi/doi/10.1261/rna.078729.121.

2003; Niswender and Conn 2010; Antflick and Hampson 2012). Several studies have implicated this receptor in multiple motor system phenotypes, neurological disorders, and disease states including learning and memory of motor tasks, spatial memory, inflammation, glucagon release, cancer progression, addiction, pain, the motor stimulatory effects of alcohol, and Parkinson's disease (PD) (Blednov et al. 2004; Uehara et al. 2004; Chang et al. 2005; Iacovelli et al. 2006; Fallarino et al. 2010; Julio-Pieper et al. 2011; Vilar et al. 2013; Niswender et al. 2016; Ponnazhagan et al. 2016; Lebourgeois et al. 2018). Despite the array of evidence demonstrating the physiologic relevance, "druggability," and pharmacologic importance of $mGlu_4$, additional information remains to be discovered regarding the regulation of this receptor. For example, it has recently been shown that RNA encoding $mGlu_4$ can undergo a post-transcriptional process known as RNA editing. Using existing RNA sequencing data sets to identify novel editing sites across the human transcriptome, Ramaswami et al. (2013) first discovered adenosine-to-inosine (A-to-I) editing of $mGlu_4$ pre-mRNA transcripts in 2013. The conversion of A-to-I is a widespread cotranscriptional modification resulting from the hydrolytic deamination of selective adenosine residues catalyzed by a family of Adenosine Deaminases that Act on RNA (ADARs) (Bass 2002). Localized to the nucleus, ADARs target select adenosines by binding to double-stranded (ds) RNA substrates, often formed via inverted repeats between exons and neighboring introns of pre-mRNA transcripts. ADAR1 and ADAR2 have been demonstrated to have an overlapping ability to edit certain adenosines, while acting specifically at others (Bass 2002; Savva et al. 2012).

Millions of poorly conserved editing sites have been discovered across mammalian transcriptomes within 5′ and 3′ regulatory elements of mRNA transcripts (Levanon et al. 2004; Li et al. 2009; Ramaswami et al. 2013); however, there is a small, select number of adenosines within coding sequences that are highly conserved across species and undergo substantial editing (Pinto et al. 2014). In the brain, these editing events occur in transcripts encoding proteins critical for neuronal signaling and excitability, including ionotropic glutamate and GABA receptor subunits, the Kv1.1 potassium channel, and the $5HT_{2C}$ serotonin receptor (Bass 2002; Rosenthal and Seeburg 2012). As inosine is read as guanosine by the cellular translational machinery, these A-to-I editing events often result in nonsynonymous codon changes in mRNA, resulting in the production of proteins with altered amino acid sequences and potentially unique functional properties.

A-to-I editing of $mGlu_4$ transcripts predicts the substitution of an arginine at position Q124; this amino acid resides within the critical "helix B" of the amino-terminal, glutamate binding domain of the receptor (Kunishima et al. 2000). mGlu receptors are obligate dimers, and helices B and C are critical in forming the mGlu dimer interface in both the resting and activated states of the receptor (Kunishima et al. 2000; Tsuchiya et al. 2002; Muto et al. 2007; El Moustaine et al. 2012; Koehl et al. 2019). mGlu receptors are obligate dimers and several studies have demonstrated the importance of helix B in modulating receptor dimerization, trafficking, and activation (Sato et al. 2003; El Moustaine et al. 2012; Levitz et al. 2016). Additionally, while once thought to only homodimerize, recent in vitro and ex vivo studies suggest the formation of heterodimeric mGlu receptors that respond to select agonists and allosteric modulators with unique pharmacologic profiles compared to homodimers formed from either protomer alone (Doumazane et al. 2011; Kammermeier 2012; Levitz et al. 2016; Niswender et al. 2016; Moreno Delgado et al. 2017; Habrian et al. 2019; Lee et al. 2020; Xiang et al. 2021). The propensity for homo- or heterodimerization is largely determined by the interactions between the extracellular amino-terminal domain of two protomers which contains the dimer interface and, in $mGlu_4$, the editing site (Levitz et al. 2016; Lee et al. 2020). While the existence of the Q124R editing site in $mGlu_4$ transcripts has been known for several years, no studies to date have addressed questions surrounding its regulation or function. The present analysis was designed to fully identify and quantify editing sites within the $mGlu_4$ ligand-binding domain, describe the *cis* and *trans* elements involved in the regulation of this event within the mammalian brain, and explore the functional consequences of editing in the $mGlu_4$ receptor.

RESULTS

A-to-I editing alters two amino acids in the $mGlu_4$ dimer interface

RNA-seq is a powerful tool to identify and quantify A-to-I editing sites across the transcriptome. However, low read depth for certain transcripts can lead to a failure to detect less frequently edited adenosines as well as improperly quantify those detected. We scanned the rat $mGlu_4$ coding sequence using Sanger sequencing for evidence of RNA editing; however, artifacts, or "noise," observed by Sanger sequencing may be mistaken for evidence of RNA editing. Therefore, we used a targeted approach, high-throughput multiplexed transcript analysis (HTMTA) (Morabito et al. 2010b), to validate potential editing sites observed by Sanger sequencing methods occurring within regions encoding amino-terminal domain of the receptor. Using HTMA, we probed rat (NM_022666.1) $mGlu_4$ transcripts from nucleotides 1022–1108, 1221–1330, 1339–1459 (encoding T50–D92, V123–V165, A166–V198) for novel editing sites. Reads were restricted due to read length limitations of the Illumina sequencing platform. After validating two editing sites which lay within the sequence encoding a putative dsRNA editing substrate in

rat mGlu$_4$ transcripts, the homologous region of human transcripts (NM_000841.4) from nucleotides 729–854 (encoding P93–R135) was probed. Using this technique, we quantified the editing levels of the Q124R editing site in multiple brain regions of both rat (~27.6%) and human (~10.3%) tissues (Fig. 1A,B). In addition to this previously discovered Q124R site, we identified a novel editing site located 15 nt downstream from this position (editing percentages in brain of 1.6% rat, 2.1% human), predicting a lysine to arginine substitution at position 129 of the resulting protein (Fig. 1A). No additional sites were observed in human transcripts across predicted RNA duplex regions (Data not shown).

Together, transcripts edited at these two sites comprise roughly ~11.7% and 22.3%–35.1% of the transcript pool in human and rat brain samples, respectively. Using HTMTA, we identified and quantified the 4 unique transcript isoforms resulting from editing at all combinations of the two sites (Fig. 1B). Edited transcript levels appeared region-specific in the rat brain, with editing levels in cerebellum and hypothalamus varying significantly from cortex, hippocampus, and striatum. Though the Q124R transcript isoform was the most prevalent edited transcript in all rat brain regions, levels were 10%–11% higher in the cerebellum and hypothalamus than in the cortex ($P < 0.02$) and striatum ($P < 0.01$). K129R and Q124R/K129R transcripts were likewise increased 0.17%–0.25% in hypothalamus ($P < 0.05$) compared to cortex and hippocampus and increased 0.97%–1.2% compared to all other regions ($P < 0.0001$), respectively. Conversely, these transcripts were

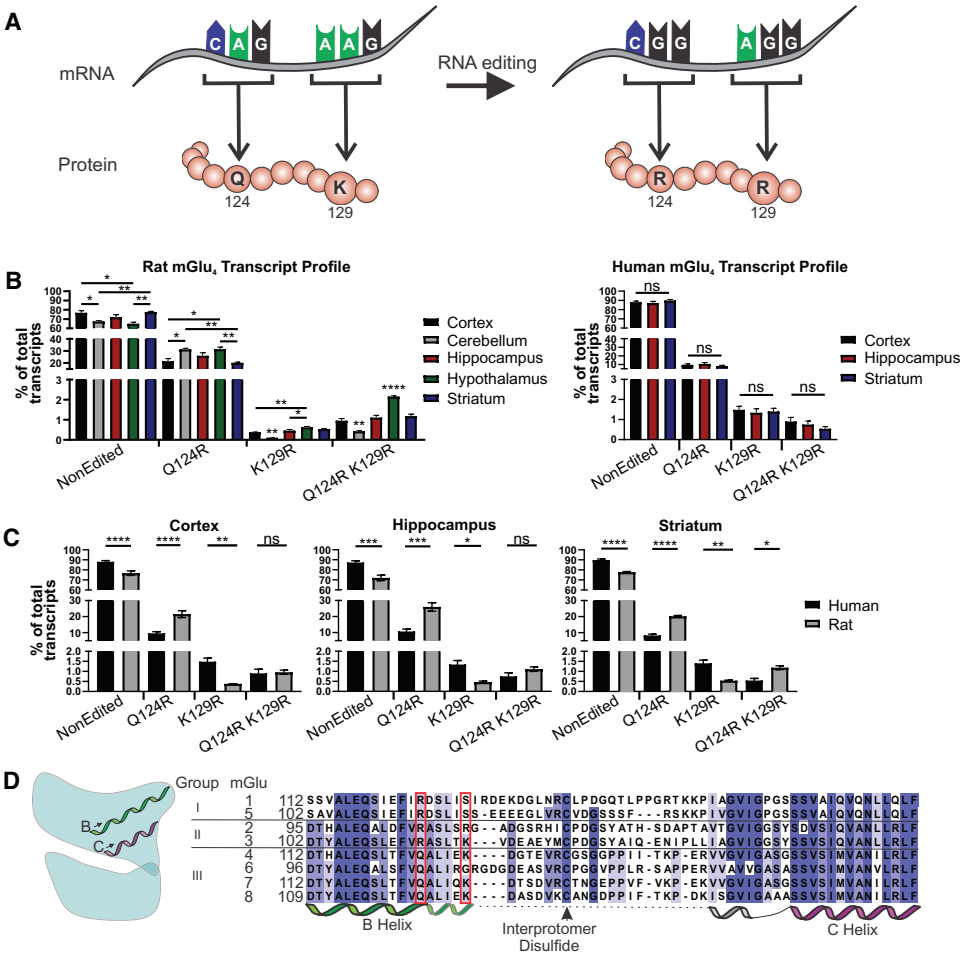

FIGURE 1. A-to-I editing of mGlu$_4$ transcripts reveals conservation of editing between rodents and humans. (*A*) Cartoon depiction of mRNA codons altered by RNA editing and their predicted translation by the ribosome. Editing is depicted as changing an adenosine to guanosine because A-to-I editing is functionally an "A" to "G" conversion for the ribosome. (*B*) Transcript isoforms expressed as a percentage of the total mGlu$_4$ transcript pool. Mean ± S.E.M. Significance tested by one-way ANOVA with Tukey's post hoc test (ns, $P > 0.05$; [*] $P \leq 0.05$; [**] $P \leq 0.01$; [***] $P \leq 0.001$; [****] $P \leq 0.0001$, rat $n = 3$, human $n = 6$–8). (*C*) Replot of the data in *B* to highlight the differences in human and rat brain regions. Mean ± S.E.M. Significance tested by one-way ANOVA with Sidak's post hoc test. (*D*) Editing alters two amino acids (Q124R, K129R) highlighted in red within the B helix of the ligand binding domain. The helices of both monomers come together to comprise the mGlu dimer interface. Helix B and C are denoted *below* the alignment. The portion of helix B which is maintained in both active and inactive receptor states is outlined in black *below* the alignment. The helix without outline represents the amino acids incorporated into helix B in the relaxed state of the receptor.

significantly decreased in cerebellum, with 0.27%–0.52% lower levels of K129R transcripts compared to cortex or hippocampus ($P < 0.02$) and 0.53%–0.76% Q124 K129R in cerebellum compared to all other tissues ($P < 0.01$). For both human and rat samples, no significant differences were found between the levels of edited transcripts in cortex, hippocampus, and striatum within species (Fig. 1B). Interestingly, while Q124R edited transcripts were on average 2.7-fold higher (16.5%, $P < 0.0001$) in rat brain regions compared to human, the opposite was true for those edited at K129R alone, which was 2.9-fold higher (0.9%, $P = 0.04$) in human transcripts. In contrast, transcripts edited at both sites were not significantly different between species in the hippocampus and cortex but showed a significant 2.2-fold increase (0.64%, $P = 0.02$) in rat striatum (Fig. 1C).

RNA editing of $mGlu_4$ transcripts predicts the substitution of amino acids within the B helix of the resulting receptor protein (Fig. 1D). An alignment of the mGlu receptors' B and C helix peptide sequences from rat (Fig. 1D) and human sequences (data not shown) reveals that the B helix is well conserved across the mGlu receptors as well as across species. Q124 of $mGlu_4$ is completely conserved in group III mGlu receptors; however, an arginine is present in the group I and II mGlu receptors. K129 of $mGlu_4$ is conserved in group III receptors, except for $mGlu_6$, but is less conserved than the Q124 position across the mGlu receptor family.

Co-regulation of multiple editing sites in $mGlu_4$ transcripts

The serotonin $5HT_{2C}$ receptor contains five editing sites (A, B, E, C, D) closely interspaced within a single RNA duplex (Burns et al. 1997; Wang et al. 2000). Previous studies have suggested that a correlation between editing at these sites demonstrates a co-regulation either of multiple sites within the same transcript or across different brain regions (Carmel et al. 2012; O'Neil et al. 2017). Given the proximity of the $mGlu_4$ editing sites, we hypothesized that the Q124R and K129R sites could be regulated by a similar mechanism. In both human striatum ($r = 0.80$, $P = 0.03$) and hippocampus ($r = 0.75$, $P = 0.03$), the levels of Q124R editing were predictive of the extent of editing at K129R within the same subject (Table 1; Fig. 2A), consistent with these sites being co-regulated in these tissues, possibly controlled by a similar mechanism that determines the extent of editing at both sites. Interestingly, this correlation was not significant in the cortex. In addition, the total extent of $mGlu_4$ editing in the striatum correlated with the total extent of editing in the hippocampus, suggesting a potentially similar regulation of editing of the $mGlu_4$ substrate within these two brain regions ($P = 0.036$) (Table 1; Fig. 2B); in contrast, a significant correlation was not observed between the extent of editing in the cortex and either striatal or hippocampal regions. This correlation was not significant when examining the extent of editing of either the Q124R or K129R sites alone; however, this is likely due to a limited samples size, and comparisons of editing in human striatal and hippocampal samples at Q124R ($P = 0.055$) and K129R ($P = 0.051$) sites approached statistical significance. These results suggest not only that the extent of editing of the Q124R and K129R sites may be co-regulated within a particular brain region, but that regulation may be distinct in other tissues.

The $mGlu_4$ RNA duplex is entirely exonic

An extended RNA duplex is essential for ADAR binding and catalytic A-to-I conversion. Using the protein folding algorithm *mfold*, a putative fold was generated using 9000 base pairs of the $mGlu_4$ human pre-mRNA sequence (NC_000006.12) surrounding the editing sites. A similar fold was generated using rat mRNA sequence (NM_0226666_1) by constraining the input sequence to that of the putative duplex in human mRNA (Fig. 3A). The Rattus norvegicus $mGlu_4$ mRNA sequence attained from NCBI (NM_022666.1) contained a (CGG) codon while the genomic reference (AC_000088.1) for the same species denotes a (CAG) codon for amino acid 124 of the receptor. We believe that an edited mRNA sequence was submitted in this case. Folds were developed using this sequence after modification of the (CGG) codon to (CAG).

TABLE 1. Pearson correlation and linear regression analysis summary table

		Pearson			Linear regression		
Edit site	Tissue	*R*	R^2	*P*	R^2	Slope	*P*
Q124R vs. K129R	Cortex	0.645	0.416	0.167	0.416	2.100	0.167
	Hippocampus	0.751	0.565	0.032	0.565	3.632	0.032
	Striatum	0.803	0.644	0.030	0.644	2.881	0.030
Total $mGlu_4$ editing	Ctx vs. Hipp	−0.031	0.001	0.954	0.001	0.229	0.954
	Str vs. Hipp	0.787	0.619	0.036	0.619	0.408	0.036
	Ctx vs. Str	−0.034	0.001	0.956	0.001	−0.027	0.956

This table contains the values of analysis shown in Figure 2.

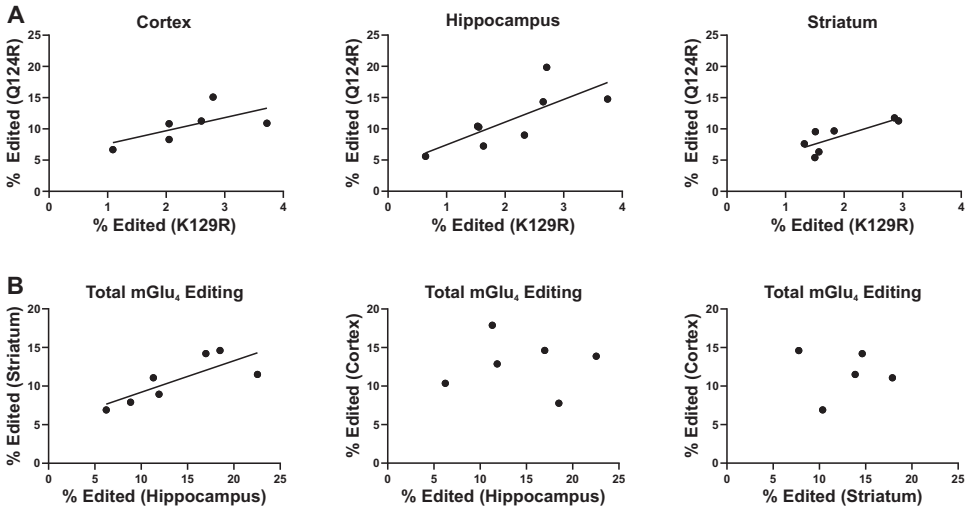

FIGURE 2. Co-regulation of human $mGlu_4$ editing. (*A*) Pearson correlation of total editing of the Q124R site versus the K129R site within individuals. (*B*) Correlation of total editing levels between distinct brain regions of individual subjects.

Surprisingly, these studies predicted putative 127 bp folds containing both editing sites which were composed entirely of exonic sequence. The majority of validated RNA editing substrates are comprised of inverted repeats between exons and neighboring introns. These putative folds agreed with the observation that human and rat $mGlu_4$ cDNA constructs, which lack intronic elements, were edited at both Q124R and K129R positions when cotransfected with ADAR enzyme constructs in HEK293T cells (Fig. 3B). To validate the putative rat RNA duplex, the minimal sequence encoding the putative duplex was expressed as a minigene either alone or when cotransfected with ADAR cDNA constructs in HEK293T cells (Fig. 3C). This minimal sequence was sufficient for editing of both sites and the specificity of editing by ADAR1 and ADAR2 was consistent with the results for full length cDNA transcripts. There are two splice isoforms of ADAR1, p110 and p150. Only the constitutively expressed ADAR1 p110 was used for analysis as it serves as the primary splice isoform of editing within the central nervous system (CNS), whereas interferon-inducible ADAR1p150 is a crucial regulator within the innate immune response (Pestal et al. 2015). These splice variants share identical deaminase and double-stranded RNA binding domains both of which confer the specificity and efficiency of the enzyme (Wong et al. 2001). ADAR3 was excluded from analysis as it has not been shown to be catalytically active. As expected in cells that do not endogenously express editing enzymes (Herb et al. 1996; Melcher et al. 1996a,b; Ohlson et al. 2007), there was no editing observed when minigene constructs were cotransfected with an empty vector control (Fig. 3B,C), demonstrating that any editing observed was due to the cotransfected ADAR construct.

"Compensatory" or "destabilizing" mutations were designed either adjacent to or across from the editing sites within the proposed duplex; either set of mutations alone was predicted by *mfold* to destabilize the RNA secondary structure, whereas minigenes with both destabilizing and compensatory mutations were predicted to fold similarly to the wild-type construct. Consistent with a destabilized structure preventing ADAR binding, no editing was observed in constructs with "destabilizing" or "compensatory" mutations alone by either ADAR1 or ADAR2. Editing was rescued in the restabilized structure bearing both destabilizing and compensatory mutations, with similar ADAR specificity when compared to the wild-type minigene. No significant differences were detected between the extent of editing at either site by ADAR1 in the wild-type and restabilized minigene. ADAR2-meditated editing of the Q124R site was rescued to ~70% of the levels seen in the wild-type duplex; this incomplete rescue is likely due to alterations in the nucleotide sequence which, along with the critical requirement of RNA secondary structure, determine site-selective editing (Polson and Bass 1994; Eggington et al. 2011).

The $mGlu_4$ RNA structure is conserved in multiple mammalian species

Transcripts encoding additional members of the group III mGlu receptors, rat $mGlu_6$, rat $mGlu_7$, and $mGlu_8$, share 74.8%, 75.0%, and 74.2% nucleotide identity, respectively, across the predicted rat $mGlu_4$ duplex region. These transcripts all share the Q124 (CAG) codon while $mGlu_7$ and $mGlu_8$ also share the K129 (AAG/AAA) codon (Fig. 4A). Analysis of the rat $mGlu_6$, $mGlu_7$, and $mGlu_8$ RNA sequences in *mfold* failed to generate extended RNA duplex structures similar to that of $mGlu_4$. No editing was observed at either codon (Fig. 4B) in $mGlu_7$ or $mGlu_8$ transcripts amplified from rat hippocampus. In contrast to the lack of

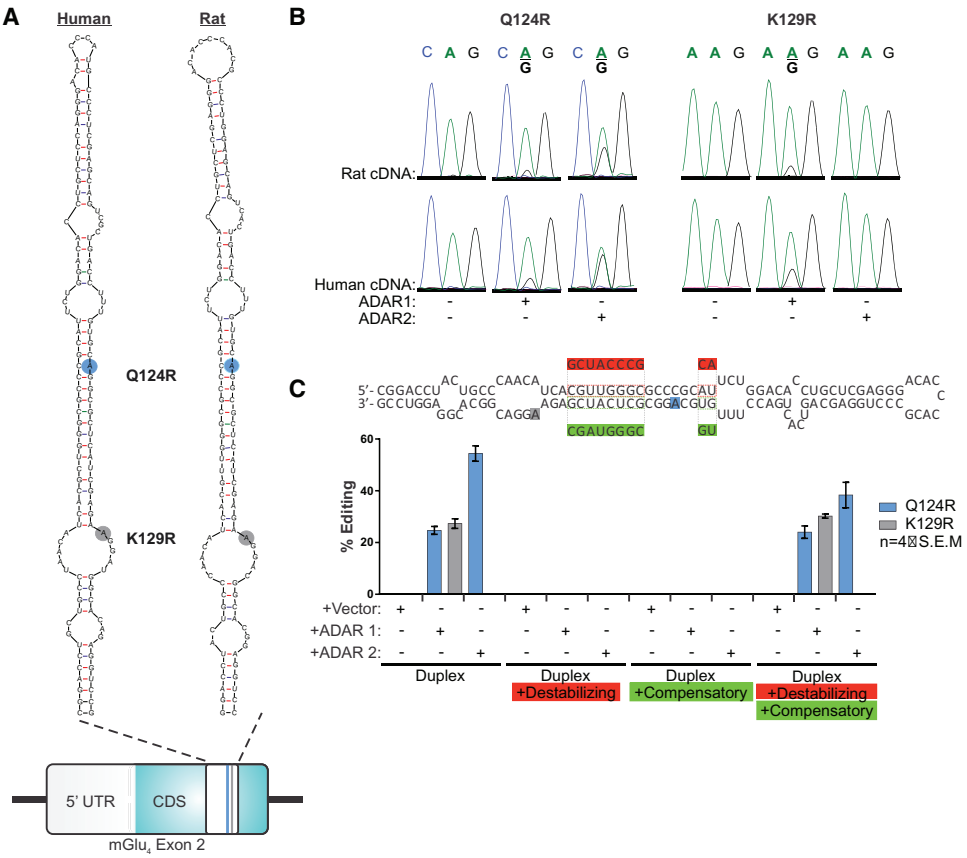

FIGURE 3. An mGlu$_4$ RNA duplex composed of exonic sequence is sufficient for editing. (*A*) Predicted mGlu$_4$ RNA duplex generated using *mfold*, composed of nucleotides 729–855 (Human, NM_000841.4), and 1132–1258 (Rat, NM_022666.1). (*B*) Editing of rat and human cDNA constructs cotransfected into HEK293T cells with either empty vector, ADAR1, or ADAR2. Editing can be seen by the dual "A" and "G" chromatogram peaks. (*C*) Predicted rat mGlu$_4$ duplex expressed as a minigene cotransfected into HEK293T cells ± ADAR1, ADAR2, or vector control. Editing percentages are calculated by measuring the peak heights of Sanger sequencing chromatogram peaks. Mean ± S.E.M. $n = 4$. Q124R and K129R editing site positions within the duplex are denoted by blue and gray colors, respectively. The nucleotide sequence on the opposing side of the proposed duplex to the editing site (outlined in red hashes) was mutated (mutant sequence highlighted solid red) to destabilize the structure. The nucleotide sequence surrounding the editing site (outlined in green) was mutated (mutant sequence in solid green) with compensatory changes to restabilize the RNA duplex.

conservation of editing among the group III mGlu receptors, the mGlu$_4$ duplex region is highly conserved among species, with sequences sharing 78.0%–100% nucleotide identity with human transcripts within this region of the mRNA. This high level of sequence conservation among species is not surprising, as exonic sequences are often highly conserved; however, extended duplex structures resembling the human and rat duplex were observed for some, but not all, species using *mfold* (Fig. 4D). Folds were highly conserved for mammals but not reptiles, suggesting that editing of mGlu$_4$ transcripts evolved in a common ancestor of mammalian species. This agrees with the suggested model that RNA editing begins with the formation of a basic secondary structure, followed by small variations that lead to the generation of species-specific editing levels and, in some cases, additional species-specific sites (Reenan 2005). Editing has been shown to be conserved in multiple mammalian mGlu$_4$ transcripts including human (Fig. 1A), macaque (O'Neil et al. 2017), rat (Figs. 1A, 3B), and mouse (Licht et al. 2019) brain samples (Fig. 4C,D).

Editing of both dimer subunits does not alter $G_{i/o}$ activation

The Q124 residue within the B helix is situated on the exposed outer face of the amino-terminal domain, removed from the core ligand binding pocket. Therefore, Q124R substitution was not expected to alter orthosteric agonist binding; however, it was predicted to potentially stabilize the dimer interface within the active state of the receptor when present in both protomers. Therefore, we empirically determined if editing induced nonsynonymous amino acid substitutions that would alter the response to orthosteric agonists. We expressed nonedited, Q124R, K129R, and Q124R/K129R isoforms alone in HEK293 cells, which do not endogenously express mGlu$_4$, and measured receptor

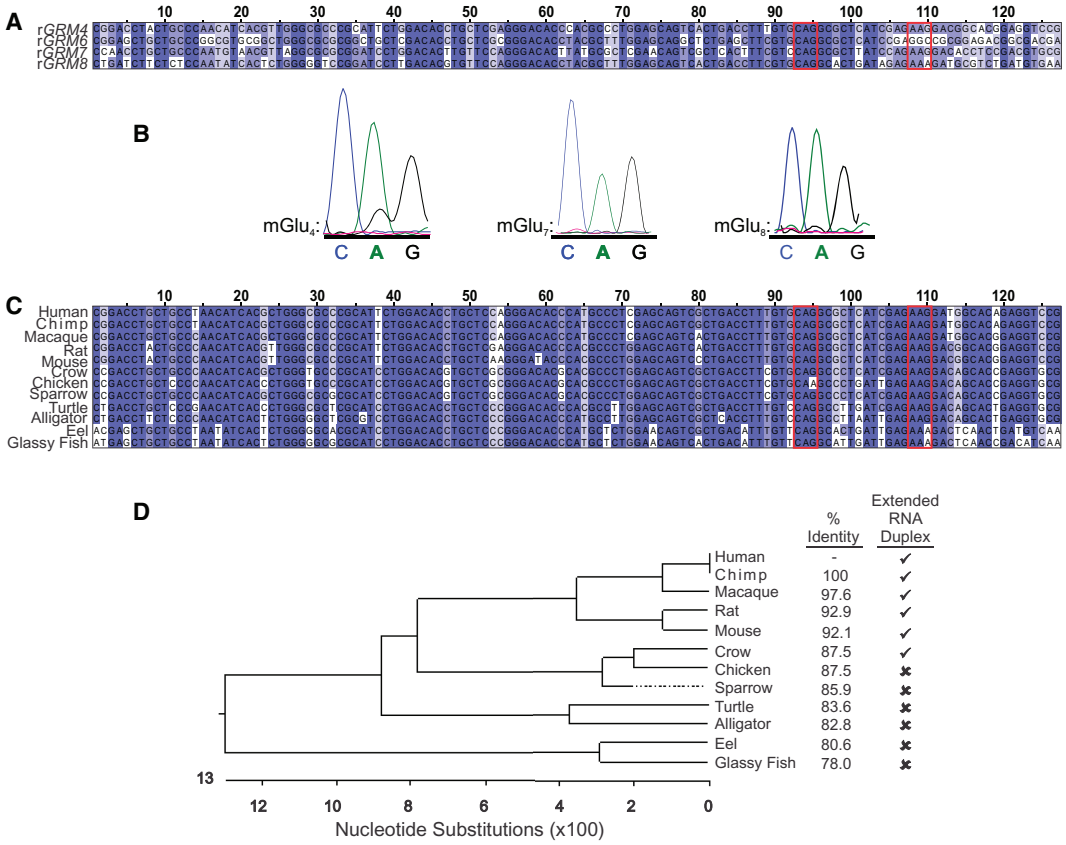

FIGURE 4. Mammalian conservation of the $mGlu_4$ duplex. (*A*) Alignment of rat $mGlu_6$, $mGlu_7$, and $mGlu_8$ mRNA sequences to the $mGlu_4$ duplex. (*B*) Sanger sequencing data demonstrating a dual adenosine and guanosine chromatogram peak characteristic of RNA edited transcripts in $mGlu_4$ samples amplified from rat cerebellum but not $mGlu_7$ or $mGlu_8$ transcripts amplified from rat hippocampus. (*C*) Alignment of the $mGlu_4$ duplex across multiple species. Q124R and K129R codons altered by editing are outlined in red boxes. Nucleotides are colored by percent conservation. Darker blue represents higher % conservation of the highlighted nucleotide. Conservation demonstrated in four groups from darkest blue to white (>80%, >60%, >40, <40%). (*D*) Cladogram of $mGlu_4$ duplex sequence generated using DNAstar software (DNASTAR Inc.). Percent identity is shown in comparison to the human sequence. Sequences producing a similar extended RNA duplex to human are noted by a check mark.

activity via coexpressed G Protein Inwardly Rectifying Potassium Channels (GIRK). This strategy should generate surface-expressed mGlu dimers that are composed of two identical $mGlu_4$ protomers. A thallium flux assay was used to assess the activation of the heterotrimeric G protein, $G_{i/o}$. In this assay, mGlu receptor activation is indirectly accessed by the activation of GIRK channels through dissociated βγ subunits of the activated $G_{i/o}$ heterotrimeric G-protein, increasing the rate of entry of extracellularly applied thallium influx and accumulation of intracellular fluorescence of a thallium sensitive dye. In response to agonist, no significant differences were detected between any of the receptor variants expressed alone (Fig. 5A,B). In addition, all $mGlu_4$ edited isoforms appeared to respond identically to the $mGlu_4$-specific positive allosteric modulators (PAMs) ADX88178 and VU0155041.

The Q124R site was edited to a much greater extent than the K129R site in humans and rats (Fig. 1B) and was edited by both ADAR1 and ADAR2 (Fig. 3B,C); transcriptomic studies have revealed that ADAR2 is the primary editing enzyme of highly conserved recoding sites within mammalian transcripts whereas ADAR1 specific sites are not as conserved (Tan et al. 2017; Chalk et al. 2019; Costa Cruz et al. 2020). For this reason, we focused our studies on the functional effects of the Q124R substitution. In HEK293-GIRK cells stably expressing either rat nonedited or Q124R $mGlu_4$ isoforms, the edited receptor responded identically to its nonedited counterpart in response to a battery of seven unique $mGlu_4$ agonists, including the endogenous ligands glutamate and L-SOP as well as several synthetic ligands. Potency (pEC_{50}) values obtained for each agonist displayed a nearly perfect correlation with an $R^2 = 0.9936$ ($P < 0.0001$) between the edited and nonedited receptors. These receptors likewise responded identically to several $mGlu_4$-specific PAMs and partial agonists, again demonstrating a near perfect correlation in the leftward fold shift of the agonist response for both L-AP4 ($R^2 = 0.9726$, $P < 0.0001$) and glutamate ($R^2 = 0.9969$, $P < 0.0001$) when pretreated with one of seven unique compounds (Table 2; Fig. 5C).

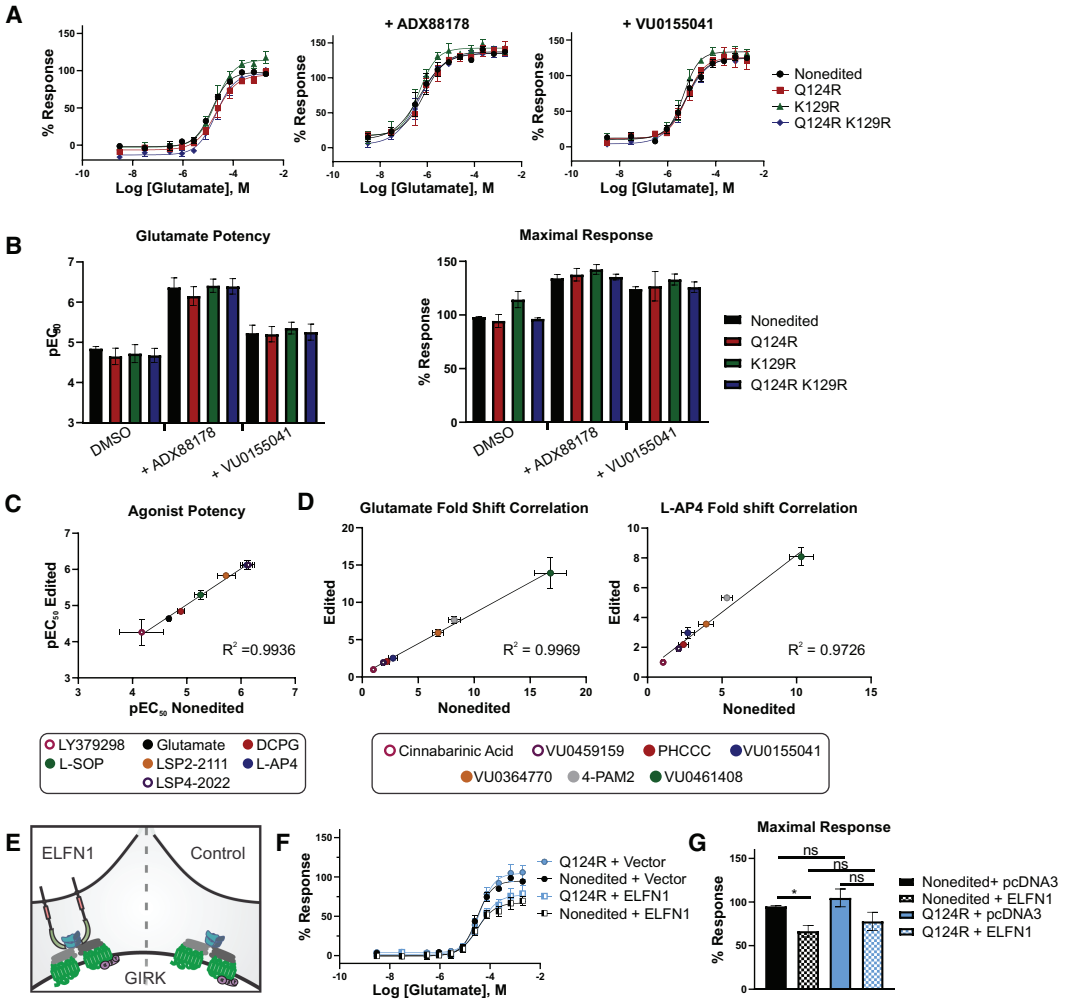

FIGURE 5. Comparison of signaling and ELFN1 interactions of edited and nonedited mGlu$_4$ receptors. (*A*) Twelve-point concentration-response curves to glutamate ± the PAM VU0155041 (30 µM) or ADX88178 (30 µM), measuring thallium flux induced by mGlu$_4$ nonedited and edited isoform activation after transient transfection into HEK-GIRK cells. Mean ± SEM. $n = 3$. Blank (WT vehicle signal) was subtracted from all values and normalized to Nonedited DMSO max response. Analyzed by one-way ANOVA. (*B*) pEC$_{50}$ and maximal response values from the nonlinear regression curves shown in *A*. Linear regression analysis of the potency and fold shift (pEC$_{50}$) of various mGlu$_4$ (*C*) agonists and (*D*) PAMs in polyclonal cells expressing either nonedited or Q124R edited mGlu$_4$ receptor. (*E*) Schematic representation of the coculture assay used to measure allosteric modulation of receptor isoforms by ELFN1. (*F*) Concentration-response curves for cells expressing mGlu$_4$ edited isoforms cocultured with ELFN1 or control cells. $n = 4$. Mean ± S.E.M. (*G*) Maximal receptor response of data represented in *F*. Analyzed by paired *t*-test between vector control versus ELFN1 for nonedited or Q124R mGlu$_4$.

Allosteric modulation by the transsynaptic ELFN1

Receptors in neurons do not exist in isolation. Synapses are highly structured environments with accessory proteins modulating the trafficking, localization, and activation of synaptic receptors. The postsynaptically expressed protein ELFN1 (Extracellular Leucine Rich Repeat and Fibronectin Domain III Containing 1) interacts specifically with, and allosterically inhibits agonist-induced efficacy of, group III mGlu receptors (Dunn et al. 2018). ELFN proteins act transsynaptically to allosterically modulate presynaptic mGlu receptors through their extracellularly exposed amino-terminal domain, which is composed of two subdomains: the cysteine rich domain (CRD) and the amino-terminal domain that binds orthosteric agonist. Due to the location of the editing sites within the extracellular mGlu$_4$ amino-terminal domain, we hypothesized that these alterations could change interaction or modulation of various edited isoforms by transsynaptic proteins. We used a coculture assay using HEK293-GIRK cells stably expressing either rat nonedited or Q124R mGlu$_4$ isoforms (Fig. 5E). The maximal response of the nonedited receptor was significantly decreased in response to glutamate specific to the ELFN1 condition over a vector alone control (Fig. 5F,G), suggesting the coculture conditions were sufficient for allosteric modulation of mGlu$_4$ receptors by ELFN1. The

TABLE 2. $mGlu_4$ agonist and PAM potency (pEC_{50}) and fold shift values

	Agonist						
A	Glutamate	L-AP4	DCPG	L-SOP	LSP2-1111	LSP4-2022	LY379298
Nonedited	4.67 ± 0.02	6.11 ± 0.11	4.89 ± 0.06	5.25 ± 0.10	5.72 ± 0.17	6.14 ± 0.11	4.17 ± 0.41
Edited (Q124R)	4.64 ± 0.05	6.12 ± 0.13	4.84 ± 0.08	5.30 ± 0.13	5.83 ± 0.06	6.12 ± 0.12	4.26 ± 0.36

B

			+10 μM Positive allosteric modulator					
Agonist	Isoform	DMSO	PHCCC	VU0461408	VU0155041	VU0364770	VU0459159	4-PAM2
Glutamate	Nonedited	4.74 ± 0.03	5.08 ± 0.03	5.96 ± 0.00	5.17 ± 0.03	5.57 ± 0.01	5.01 ± 0.01	5.65 ± 0.01
	Edited	4.72 ± 0.03	5.04 ± 0.03	5.86 ± 0.05	5.12 ± 0.03	5.49 ± 0.01	5.01 ± 0.02	5.60 ± 0.01
L-AP4	Nonedited	6.41 ± 0.06	6.78 ± 0.07	7.42 ± 0.07	6.83 ± 0.01	7.00 ± 0.02	6.73 ± 0.04	7.13 ± 0.09
	Edited	6.39 ± 0.04	6.73 ± 0.02	7.29 ± 0.06	6.85 ± 0.05	6.94 ± 0.03	6.67 ± 0.01	7.11 ± 0.05

This table contains the values of analysis shown in Figure 5C.

reduction in maximal response of the Q124R receptor did not reach statistical significance ($P = 0.096$). We also did not observe differences in response in the presence of $mGlu_4$-specific PAMs (data not shown).

Q124R substitution in one subunit does not alter $G_{i/o}$ activation

Q124R edited $mGlu_4$ mRNA isoforms account for ~12% and 30% of the transcript pool in humans and rats, respectively. Assuming each cell expresses mixed populations of transcripts, it is most likely that an edited $mGlu_4$ protein monomer would dimerize with a nonedited counterpart. We hypothesized that editing of only one monomer in an $mGlu_4$ receptor could alter the signaling characteristics of the resulting heterodimer. Observing specific heterodimer populations is challenging due to the presence of multiple surface-expressed receptor populations in cotransfection models. To address this, we took advantage of the quality control system of $GABA_B$ receptors, which requires two monomers with complementary carboxy-terminal coiled-coil domains to dimerize and mask the encoded ER retention motif in order to traffic to the surface. Chimeric $mGlu_4$ constructs fused with these unique tails, labeled Gb1 and Gb2, allowed for the surface expression of dimers comprised of edited and nonedited monomers while preventing surface expression of homodimer populations (shown schematically in Fig. 6A). The addition of GABA carboxy-terminal tails significantly decreased (28 ± 19%, $P = 0.029$) the maximal response to glutamate in comparison to the wild-type construct (Fig. 6B,C); however, the glutamate pEC_{50} was not significantly different between the constructs (data not shown), suggesting that the presence of GABA tails does not significantly alter function, but may mildly limit surface expression. No appreciable signal was observed when Gb1 and Gb2 tailed receptor constructs were expressed alone (Fig. 6B). Similar to the use of nonchimeric receptors, no significant differences were observed between dimer pairs with Q124R substitutions in both protomers compared to nonedited receptor homodimers. No differences in maximal responses or glutamate pEC_{50} were observed when restricting surface receptors to an edited/nonedited dimer pair (Fig. 6D–F).

$mGlu_4$ structural modeling

RNA editing of $mGlu_4$ substrates converts an encoded, conserved glutamine (Q) residue in group III mGlu receptors to the equivalently conserved arginine (R) in groups I and II (Fig. 1B). We next sought to understand how RNA editing might influence 3D protein structure. We created 3D homology models of the extracellular domains of $mGlu_4$ in active and inactive states based on x-ray crystallography and cryo-electron microscopy structures of the near full length $mGlu_5$ (Koehl et al. 2019). RNA editing altered residues at the top and outer surface of the extracellular domain. Q124 contributed to the dimer interface formed by the B helix between the two mGlu subunits (Fig. 7). This interface was composed of several highly conserved, hydrophobic residues as well as several less conserved, polar residues, with the B helix of each protomer immediately adjacent to an unstructured loop region, which contains the disulfide link between the dimers. K129 was found within the unstructured loop region in the inactive state and the end of the B helix in the active conformation, with the side chain accessible to solvent in both instances. Given that this region shows low similarity between mGlu subtypes, varying in both length and composition, we focused modeling efforts on Q124. We created homology models of the $mGlu_4$ dimer in both active and inactive states to predict the effects of amino acid substitution of Q124 by RNA editing where neither, one, or both protomers were edited.

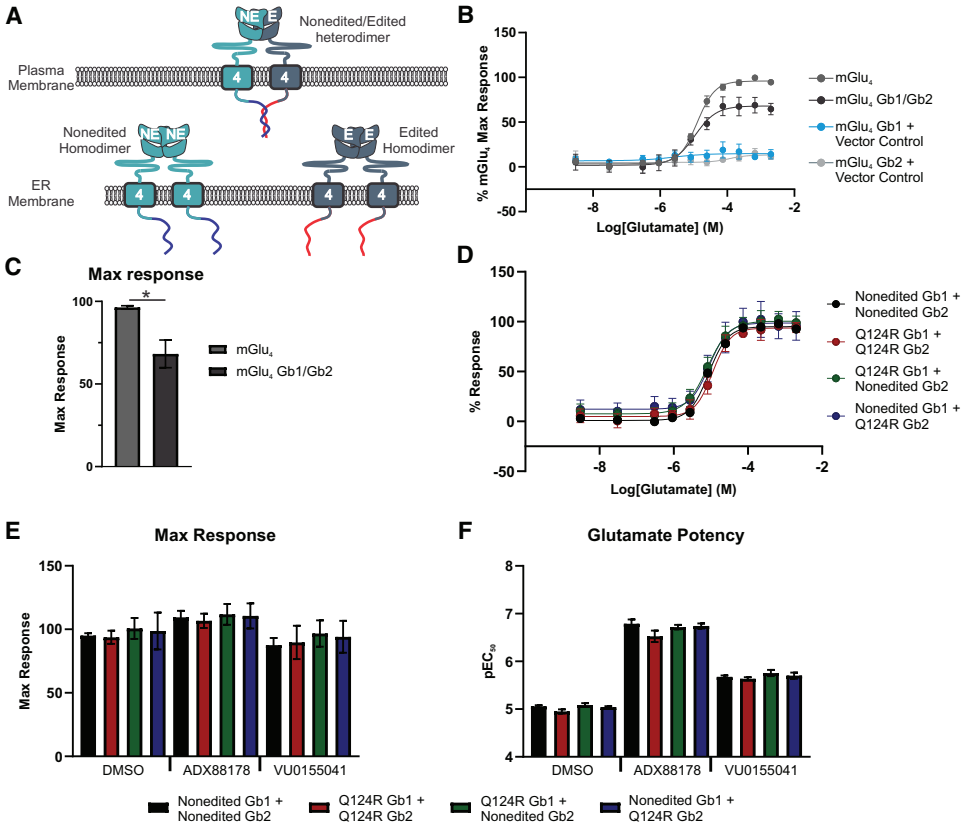

FIGURE 6. Response of edited/nonedited $mGlu_4$ receptor dimers. (*A*) Schematic representation of the use of $GABA_B$ receptor carboxy-terminal tails to restrict surface expression exclusively to heterodimers. (*B*) Concentration-response curves comparing cells transfected with equal microgram amounts of an $mGlu_4$ control construct, $mGlu_4$ $GABA_B$ tailed receptor constructs together, or tailed constructs alone plus an empty vector control. All constructs in this subfigure are nonedited at the Q124 residue. (*C*) Max response for the Gb1/Gb2 receptor combination was lower in comparison to wild-type $mGlu_4$ in the DMSO-matched condition. (*) $P \leq 0.05$; (**) $P \leq 0.01$. (*D*) Concentration-response curves for HEK293A-GIRK cells cotransfected with chimeric $mGlu_4$ constructs restricting surface dimer populations to those of two nonedited receptors or Q124R edited/nonedited receptor heterodimers. Mean ± S.E.M. $n = 3$. (*E*) Maximal response values and (*F*) glutamate potency (pEC_{50}) from the nonlinear regression curves shown in *D*. Each receptor pair is compared to the nonedited receptor condition using a one-way paired ANOVA with Sidak's post hoc analysis.

Within the active state, the positioning of Q124 at the B helix dimer interface was relatively static, with the side chain predicted to form an H bond with E128 within the same protomer (Fig. 7B). However, when one protomer was edited, the single R124 showed greater conformational diversity with the side chain having the potential to form an H bond across the dimer interface with E128 of the Q124-containing protomer (Fig. 7C). When both protomers were edited to Arg, greater conformational diversity was seen with multiple H bonding partners predicted across the dimer interface (Fig. 7D). Additionally, the Q124R substitution was predicted to alter dimer stability within the resting state. The nonedited Q124 residues were predicted to form a direct polar interaction (H-bonds) with each other between the protomers (Fig. 7B). Substitution for arginine in one protomer allowed the guanidinium group of Arg to occupy the interface between helix B/B′, with the potential to coordinate multiple polar interactions (H-bonds and salt bridges, Fig. 7C). A change of Q124R in both protomers was predicted to cause a repulsion between the two positively charged Arg residues, where neither residue was observed to occupy the interface between helix B/B′ in our molecular predictions. Therefore, we postulated that the single residue edit creates a more stable interface in the resting state, when compared to the nonedited and double Q124R edit, and that editing in both protomers would create a more stable dimer interface when the structure was in the active state. Collectively, the modeling predicted that $mGlu_4$ dimerization would likely be influenced, which may also impact heteromerization with other mGlu receptors with a Q rather than R in the homologous 124 position.

Q124R substitution decreases heterodimerization with $mGlu_2$ and $mGlu_7$

Due to the position of the editing sites along the dimer interface for mGlu receptors and based on our modeling, we

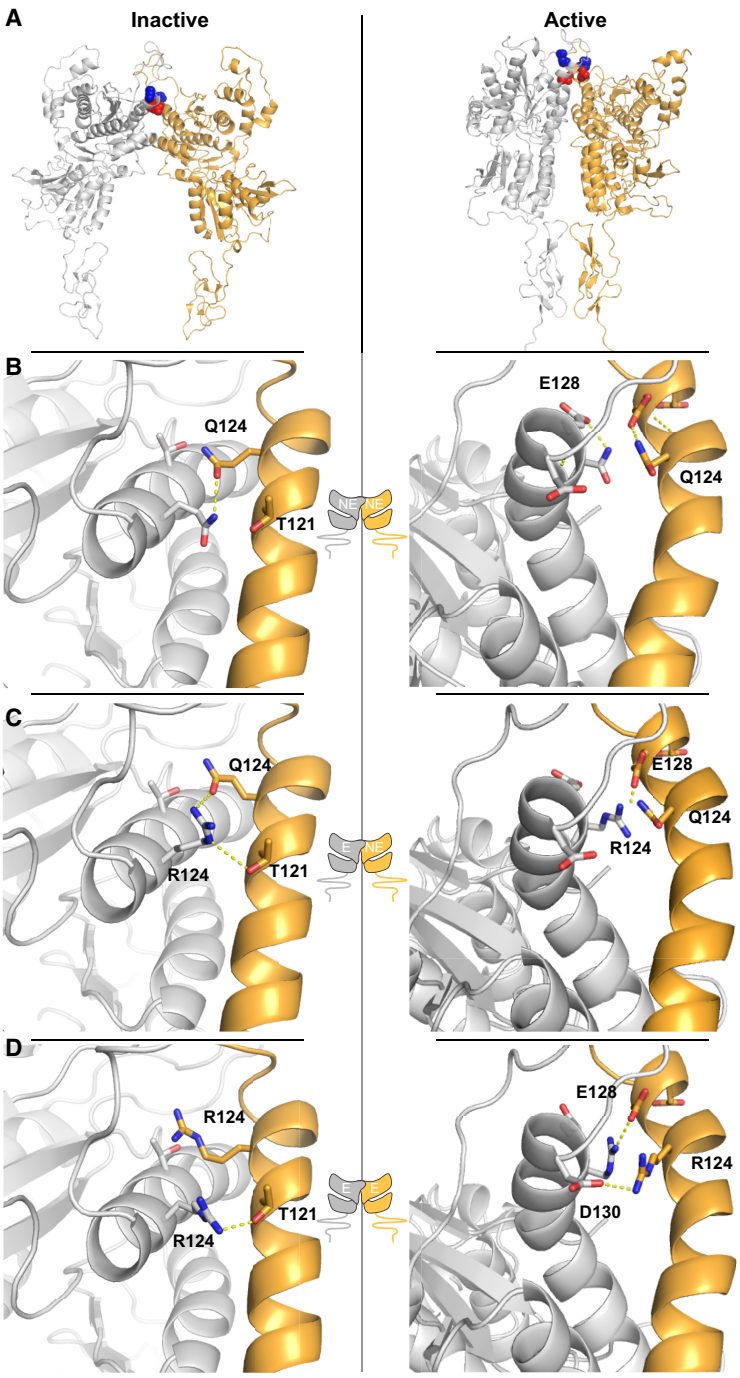

FIGURE 7. Structural modeling of the Q124R edit site in an $mGlu_4$ dimer. (*A*) $mGlu_4$ homology model of the extracellular domains based on inactive and active $mGlu_5$ structures (PDB: 6N50 and 6N4X). The positions of Q124 (red) and K129 (blue) are shown in spheres. Ribbon representation of Helix B and B′ (gold helix, all other secondary structure removed for clarity) of the opposite protomer in dimers with two nonedited protomers (*B*), a nonedited and an edited protomer (*C*), or two Q124R edited $mGlu_4$ protomers (*D*). Dashed yellow lines show potential H-bonding interactions between side chains.

sought to determine how the Q124R substitution altered the propensity of $mGlu_4$ to homodimerize versus heterodimerize with other mGlu partners. Truncating $mGlu_4$ peptides before the transmembrane domain results in a disulfide-bound $mGlu_4$ dimer that is secreted from the cell and retains similar binding affinities to its full length counterpart (Han and Hampson 1999). We took advantage of a Myc-tagged, secretable, extracellular fragment ("prey") in a cotransfection assay with a full length, HA-tagged ("bait") receptor in order to isolate and specifically measure heterodimer populations at the cell surface. In this assay, homodimer populations would be secreted and removed by washing. Heterodimer populations at the surface could then be measured specifically using unique epitope tags on the amino termini of "bait" and "prey" receptors (Fig. 8A). Both nonedited and edited, truncated $mGlu_4$ constructs were expressed, processed, and secreted at similar levels (Fig. 8B). Cell lysates were reduced by the addition of DTT and represent monomeric $mGlu_4$ ATD constructs. "Media" blot samples have not been DTT-treated and demonstrate dimerization of the ATD constructs, shown by the bottom band of the "media" blot. The top band of the media blot may represent binding of the ATD dimer to a serum protein and is not expected to affect dimerization. Interestingly, editing of the Q124R site did not alter levels of dimerization with the full length nonedited $mGlu_4$ construct; however, a significant decrease was observed in dimerization propensity with $mGlu_2$ ($35.8 \pm 4.3\%$, $P < 0.05$) and $mGlu_7$ ($28.1 \pm 3.8\%$, $P < 0.05$) receptors. For all other mGlu receptors, the propensity to dimerize with $mGlu_4$ was unaffected by editing (Fig. 8C). It can further be seen by pooling data from heterodimer populations where editing had no effect that there is a clear order of dimerization preference for $mGlu_4$, with decreased preference for the group I receptors ($mGlu_1$, $mGlu_5$), and an increased propensity to heterodimerize with group II receptors ($mGlu_2$, $mGlu_3$) in agreement with previous studies (Fig. 8D; Doumazane et al. 2011; Lee et al. 2020). In addition, our assay included the $mGlu_8$ receptor, and $mGlu_4$

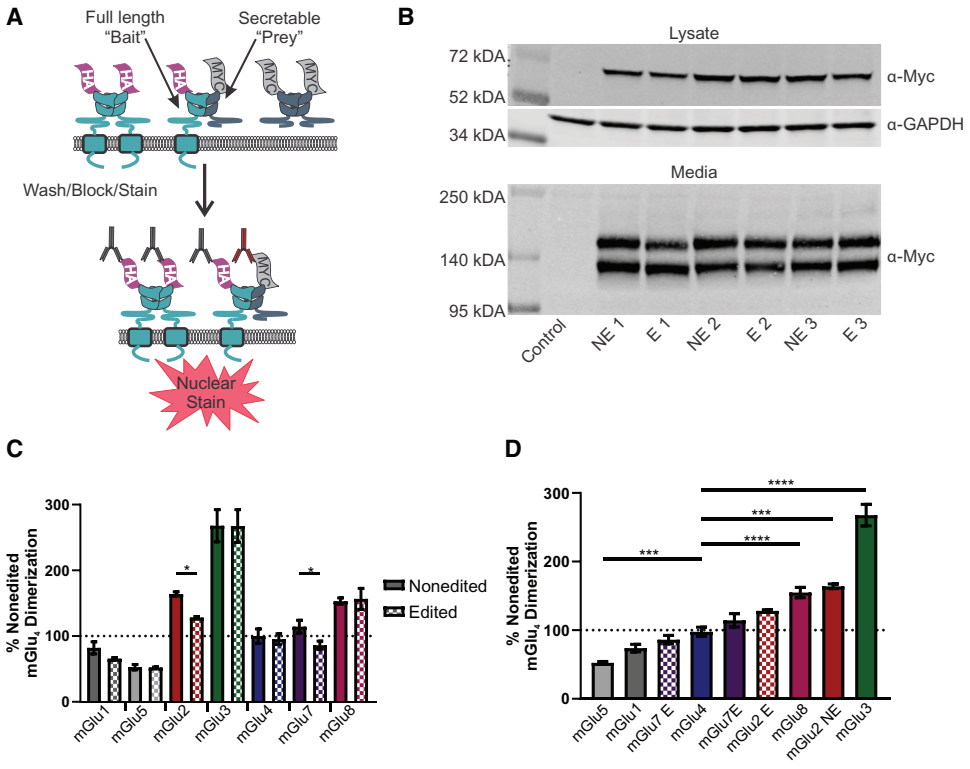

FIGURE 8. Q124R substitution decreases heterodimerization with mGlu$_2$ and mGlu$_7$. (*A*) Schematic representing the "bait" and "prey" method to measure mGlu dimerization propensity. HA or MYC signal are measured in separate wells and normalized to DRAQ5 cell stain to account for cell number. (*B*) Western blot analysis of truncated, nonedited, and edited mGlu$_4$ receptor constructs from concentrated media or whole-cell lysates. (*C*) mGlu$_4$ dimerization propensity assessed by the ratio of the secretable mGlu$_4$ (MYC) signal to full length (HA) signal. Data are normalized to the dimerization levels of nonedited mGlu$_4$. Mean ± S.E.M. Significance assessed by paired *t*-test. (*) $P \leq 0.05$. (*D*) Replot of the data in *C* after pooling data for receptors where editing did not affect dimerization showing the order of mGlu$_4$ dimerization propensity. Mean ± S.E.M. Significance assessed by ANOVA with Dunnett's post hoc. (ns, $P > 0.05$; [*] $P \leq 0.05$; [**] $P \leq 0.01$; [***] $P \leq 0.001$; [****] $P \leq 0.0001$).

demonstrated a substantial preference for heterodimerization with mGlu$_8$ compared to homodimerization, with a significant, 57% ($P < 0.0001$) increase in the propensity to heterodimerize.

DISCUSSION

The study of RNA editing has evolved rapidly over the last decade. What was once thought to be a rare phenomenon discovered often serendipitously by comparing individual RNA and DNA sequences has transformed into high-throughput analyses determining editing patterns across entire transcriptomes. Millions of edit sites are now known to occur throughout mammalian transcripts, most of which occur in noncoding regions and are not conserved between species. While this has led to some debate in the field as to whether all RNA editing events are biologically relevant, there is a consensus that editing sites that are conserved across species and have the potential to cause nonsynonymous amino acid substitutions are functionally important and warrant further study (Levanon et al. 2004; Pinto et al. 2014; Yablonovitch et al. 2017; Chalk et al. 2019).

While the editing of mGlu$_4$ transcripts has been reported previously, this has mostly been in the context of measuring overall editing patterns of multiple substrates in large RNA-seq data sets (Ramaswami et al. 2013; O'Neil et al. 2017; Licht et al. 2019). Our analysis is the most robust, targeted HTS approach to analyze the editing of mGlu$_4$ transcripts across multiple brain regions in rat and human samples. Our data have demonstrated the existence of the novel editing site, K129R, as well as region-specific editing patterns in rat brain samples. Mean levels of editing varied significantly in hypothalamic and cerebellar regions of rat brain samples but appeared to be static in both humans and rats within the cortex, hippocampus, and striatum. While the mean levels of editing across transcripts appeared similar, correlation analysis comparing editing levels across human brain suggests more variation in region-specific editing levels within individuals, specifically in the striatum and hippocampus versus cortex, than the mean values imply. Interestingly, previous work reported that editing of the Q124R site in macaque samples was

decreased in the striatum compared to the cortex, suggesting that, while editing of this site is conserved across multiple species, the extent of editing and spatial editing patterns vary between species.

While the extent of $mGlu_4$ editing is low (~10% in human brain samples), this does not necessarily default to low importance. The Q124R site of $mGlu_4$ is one of 59 evolutionary selected sites (ESS), which, due to their high conservation of editing across species, are thought to have been conserved due to the beneficial effect of protein recoding by editing (Pinto et al. 2014). Ten of these 59 ESSs display editing levels <20% in human subjects (Pinto et al. 2014); this includes the Kv1.1 ion channel (Hoopengardner et al. 2003), the E site of the 5HT2C receptor (O'Neil et al. 2017), and the SNARE accessory protein CAPDS (Miyake et al. 2016) which have demonstrated phenotypic outcomes due to RNA editing in rodent models (Jinnah and Ulbricht 2019). The effects of RNA editing are determined not only by the extent of editing but the type of amino acid substitution. Additionally, the variance of editing levels for individual transcripts between and within unique cell subtypes remains unknown. Increased editing of transcripts within select cell types or circuits may provide a critical phenotypic function within these circuits. Ultimately, the gross phenotypic consequences and importance of $mGlu_4$ editing cannot be determined until "always edited" or "always nonedited" animal models are generated, as is common in the study of RNA editing events (Jinnah and Ulbricht 2019). Of additional note, while generally most pronounced in the CNS, RNA editing may serve a critical functional role within peripheral tissues. This has been shown to be the case with a Q-to-R transition in filamin A (FLNA) which affects cardiovascular function as shown in a murine model (Jain et al. 2018). It is possible that $mGlu_4$ editing displays a unique profile or serves a critical functional role in a particular peripheral tissue in which $mGlu_4$ is expressed, including the pancreas, stomach, gastrointestinal tract/colon, breast, bladder, skin, adrenal gland, kidney, upper respiratory tract epithelia, and dendritic cells (Brice et al. 2002; Chang et al. 2005; Fallarino et al. 2010; Xiao et al. 2019).

In addition to describing the editing profile of these transcripts, our work is the first to demonstrate the minimal RNA nucleotide sequence requirements for RNA editing of $mGlu_4$ transcripts and site-specificity of A-to-I catalysis by ADAR enzymes. The proposed intron-less structure is specific to $mGlu_4$ among the group III mGlu receptors and highly conserved across multiple mammalian species. This is only the third such editable substrate to be discovered and validated for which the RNA structure is composed entirely of exonic sequence, implying that it could be subject to editing outside of the nucleus (Bhalla et al. 2004; Ohlson et al. 2007). ADAR enzymes are normally localized to the nucleus, but certain splice variants of ADAR1 can be expressed in the cytoplasm in response to viral infection, inflammation, and interferon induction (Patterson and Samuel 1995; Poulsen et al. 2001; Desterro et al. 2003; Sansam et al. 2003). The extent of editing of RNA substrates composed of exonic and intronic sequence is highly correlated with splicing efficiency, whereas no correlation has been observed for those substrates composed entirely of exonic sequence (Licht et al. 2016). In mice, no significant correlation was observed between editing levels and splicing efficiency of $mGlu_4$ transcripts, further validating the strictly exonic sequence composition of the $mGlu_4$ RNA duplex (Licht et al. 2019). Our results show that, in vitro, both ADAR1 and ADAR2 are able to edit the Q124R site, whereas only ADAR1 can edit the K129R site. Moreover, ADAR1 can edit both Q124R and K129R sites to roughly equal extents. This is in direct contrast to the significantly higher levels of editing at the Q124R site compared to K129R observed in human and rat tissues, leading us to speculate that ADAR2 is the predominant enzyme acting on $mGlu_4$ substrates in vivo. In agreement with this hypothesis, a recent publication by Licht et al (2019) did not observe editing at the Q124R position in *Adar2*$^{-/-}$ animals (Licht et al. 2019). Additionally, Licht et al. did not identify editing at the K129R site; however, this study was performed in whole brain samples of p14 mice after enriching specifically for nascent transcripts (Licht et al. 2019). Editing sites display unique developmental increases in editing percentages and levels of K129R editing may not be observable until later developmental stages (Wahlstedt et al. 2009). Mutational disruption of base-pairing immediately 5′ and 3′ of the Q124R editing site ablated editing which was restored upon the introduction of complementary mutations which restabilized the proposed base-pairing. The duplex generated using *mfold* is a putative structure; however, these results suggest that base-pairing within the central stalk of the putative duplex surrounding the editing site is critical for A-to-I catalysis of $mGlu_4$ transcripts and that a 16 nt region ending 56 nt upstream of this region is most likely the editing complementary sequence (ECS), or RNA sequence directly opposing the editing site. Additionally, ADAR1-mediated editing of Q124R was fully rescued in the restabilized helix; however, ADAR2-mediated editing was restored to only ~70% of the levels seen in the wild-type duplex, suggesting the importance of both structural and sequence elements in editing efficiency of $mGlu_4$ transcripts by ADAR2.

The extent of editing at both sites was increased in vitro compared to the levels observed in dissected brain regions. ADAR2 edited roughly ~54.4% of Q124R codons of a rat $mGlu_4$ minigene in cotransfected HEK293T cells, while the extent of editing observed in rat tissues was ~27.6% (Figs. 1A, 3C). Likewise, ADAR1 edited 27.3% of $mGlu_4$ substrates at the K129R position in vitro, while the levels observed in rat brain regions were ~1.6%. There is a greatly reduced complexity in our in vitro system, which over expresses ADAR enzymes and minimal RNA

transcripts for duplex formation and likely lacks additional editing regulatory elements compared to mammalian neurons. This likely leads to the observed disparity in the extent of editing. Within human tissues, due to the high correlation we observed in the extent of editing at these two sites, it is plausible that editing of these substrates is regulated by a mechanism that controls the extent of editing by both ADAR1 and ADAR2.

The predicted amino acid substitutions occur within the B helix of the $mGlu_4$ receptor which, along with helix C, form the hydrophobic dimer interface of mGlu receptors —an area also critical in receptor activation (Kunishima et al. 2000; Sato et al. 2003; Muto et al. 2007; Levitz et al. 2016; Koehl et al. 2019). These helices are thought to comprise the only interface within the resting state which shifts upon activation to include additional contacts between the VFT and 7TM domains. While there are many conserved hydrophobic contacts in the mGlu dimer interface, there are several polar interactions which are less conserved across mGlu receptors, including the Q124 site of $mGlu_4$. The conservation of this residue suggests a critical functional importance of this position in the protein, but perhaps one that differs between group III and group I/II mGlu receptors. Several studies have observed that nonsynonymous substitutions induced by RNA editing generally occur in regions less conserved than average (Forni et al. 2015). Previous studies analyzing the crystallographic structure of $mGlu_1$ posit that R124, homologous to Q124 of $mGlu_4$, resides at the interface of both inactive and active receptor states. This residue sits at the carboxyl terminus of the B helix within the active state (Kunishima et al. 2000). In the resting state of the receptor, there is an extension of the helix to include additional residues such as K129 (Figs. 1B, 7A). These interdomain movements are thought to be conserved among mGlu receptors (Muto et al. 2007). In cryoEM structures of a full length $mGlu_5$ extracellular domain in the active and inactive state, Koehl et al. (2019) suggested that Arg114, homologous to Q124 of $mGlu_4$, releases from an interaction with E111 in the inactive state to interact with E121 of the active state (Koehl et al. 2019). This interaction was proposed to stabilize the active state of the receptor. No function has been suggested for the K129R site, which is edited an average of only 2.1% of human transcripts and 1.6% in rats; therefore, we decided to focus our efforts on elucidating the functional consequences of the Q124R site which is edited at 10.3% in humans and 27.6% in rats.

Facing the multitude of evidence suggesting a critical function of helix B and, specifically, of those residues homologous to Q124, it was surprising not to observe any significant differences in signaling of these edited receptor isoforms when present in either only one or both protomers of a dimer. The substitution of a glutamine for arginine is a subtle change. Both residues are capable of polar interactions; however, the arginine may form a salt bridge whereas glutamine would not. While this is generally a conservative substitution, the consequences can be severe; the Q84R substitution in Tribbles homolog 3 (TBR3) was associated with insulin resistance in human populations (Prudente et al. 2005) and R1131Q in the kinase domain of the human insulin receptor significantly reduced phosphorylation (Kishimoto et al. 1994). A similarly conservative substitution of surface exposed lysines to arginines in Green Fluorescent Protein (GFP) significantly increased protein stability (Sokalingam et al. 2012). Furthermore, mutations in this helix in $mGlu_2$ were shown in single molecule FRET studies not only to weaken the dimer interface but also increase the proportion of receptors in the active state, even in the absence of agonist (Levitz et al. 2016). $mGlu_1$ receptors with mutations in helix B displayed signaling defects despite binding [^{3}H]-quisqualate (Sato et al. 2003). Using the $mGlu_5$ structure as a guide, we modeled the $mGlu_4$ dimer to predict the effects of amino acid substitution by RNA editing. Residue 124 was predicted to make distinct binding interactions depending on the editing status of each protomer and whether the receptor was in an active or resting conformation, with the major prediction being to alter the stability of the dimer interface. This prediction was consistent with the lack of effect of RNA editing on receptor activation in response to agonist. It should be noted that the thallium flux assay measures activation of $G_{i/o}$. $mGlu_4$ has also been shown to promiscuously couple to $G\alpha_q$ in cerebellar parallel fiber-molecular layer interneuron synapses (Chardonnet et al. 2017). Apart from canonical G protein coupling, $mGlu_4$ activation has also been linked to the activation of PI3-kinase (Iacovelli et al. 2002, 2006), c-Jun NH_2-terminal kinase (JNK) (Zhang et al. 2015), and mitogen-activated protein kinase (MAPK) (Iacovelli et al. 2002; Chardonnet et al. 2017) signaling pathways. Additional studies are needed to determine whether RNA editing influences signaling of these noncanonical signaling pathways.

mGlu receptors are often coexpressed within the same neurons and can not only form homodimer receptors, but heterodimers as well, immensely increasing the potential variation and complexity of mGlu receptor signaling. Our structural model of the $mGlu_4$ receptor found that Q124R substitution within a single monomer resulted in the most stable dimer interface in the resting state. This suggests that Q124R substitution would increase the propensity for edited $mGlu_4$ protomers to dimerize with other mGlu receptors with a Q rather than R in the homologous 124 position. Contrary to our predictions, $mGlu_4$ constructs with a Q124R substitution did not show an increased propensity to dimerize with nonedited $mGlu_4$ protomers, which have a Q at position 124, in our dimerization assay (Fig. 8C).

Our results suggest that Q124R substitution in $mGlu_4$ decreases the receptors' propensity to heterodimerize specifically with $mGlu_2$ and $mGlu_7$, which have an encoded R and Q, respectively, at the homologous position

(Fig. 1D). Additionally, the structural model suggests residue 124 can interact with Glu128 or Asp130 of the opposite $mGlu_4$ protomer. Alignment of the helices comprising the dimer interface from all mGlu receptors shows the subtype-specific amino acids that are implicated in the dimer interface (Fig. 1D). Residues unique to $mGlu_2$ and $mGlu_7$, which cause altered dimerization propensity with edited $mGlu_4$ constructs, are not readily apparent, although altered interactions across the dimer interface with $mGlu_4$-Q124R involves nonconserved residues. It is likely, however, that dimer formation occurs in the ER while each protomer is in a pre/semifolded state, limiting the utility of using such structural comparisons to understand these data (Robbins et al. 1999).

Both $mGlu_2$ and $mGlu_7$ are expressed presynaptically and have been shown to colocalize with $mGlu_4$ (Bradley et al. 1999; Kosinski et al. 1999; Yin et al. 2014; Lee et al. 2020). $mGlu_{2/4}$ heterodimers have been documented in vitro and in vivo, with heterodimerization altering the receptors' responses to endogenous and synthetic orthosteric agonists as well as allosteric modulators (Doumazane et al. 2011; Yin et al. 2014; Moreno Delgado et al. 2017). Additionally, it has long been postulated that $mGlu_4$ and $mGlu_7$, based on their overlapping expression within striatopallidal projections (Bradley et al. 1999; Kosinski et al. 1999), could form heterodimers within this region and have been shown to interact in vitro (Doumazane et al. 2011; Lee et al. 2020). Additional studies are needed to determine whether $mGlu_{4/7}$ heterodimers exist in vivo as well as the effect of this heterodimerization on downstream signaling in response to endogenous and synthetic ligands.

In extensive modeling by the Levitz laboratory, it was suggested that, for heterodimers to occur, two mGlu receptors must have either equal or increased propensity for heterodimerization as for homodimerization (Lee et al. 2020). Further, the proportion of homo- versus- heterodimer populations present in a cell expressing two or more mGlu receptors was relatively stable across multiple molar concentration of those receptors but highly dependent on the K_d of their interaction. Heterodimerization of $mGlu_4$ with $mGlu_2$ and $mGlu_7$ was decreased by 28%–30%, which could alter the proportion of select heterodimer populations at the surface while increasing the proportion of homodimeric population. This could be especially important in cells expressing more than two mGlu receptors; in single-cell RNA sequencing (scRNAseq) analysis of mouse cortex, over 50% of glutamatergic neurons expressed at least four to five mGlu receptors and at least two to three mGlu receptors were expressed in GABAergic neurons (Lee et al. 2020). We found that nonedited $mGlu_4$ exhibited similar levels of dimerization with $mGlu_2$ and $mGlu_8$; however, editing decreased dimerization with $mGlu_2$ but not $mGlu_8$, potentially switching the preference for $mGlu_4$ dimerization ($mGlu_{4\ (NonEdited)/2} > mGlu_{4/8} > mGlu_{4\ (edited)/2}$). We also found that $mGlu_4$ and $mGlu_7$ had similar levels of dimerization, again with editing of $mGlu_4$ decreasing heterodimerization with $mGlu_7$ but not homodimerization with $mGlu_4$ subunits. Of note, this assay was carried out in a condition of either entirely nonedited or entirely edited $mGlu_4$ constructs. The effect on dimerization within cells expressing both constructs at varying percentages would likely be more subtle, but also more attunable to the cell's specific needs. Additionally, studies have reported background levels of dimerization of $mGlu_4$ with $mGlu_1$ and $mGlu_5$ (Doumazane et al. 2011; Lee et al. 2020). Levels of dimerization observed within our assay may, therefore, represent an increased background above other assay formats, although the order of dimerization propensity is similar to those previously published.

Editing is dynamically regulated by neuronal stimulation, hypoxia, stress, and energy/nutrient status, suggesting neurons can potentially modulate their editing status in response to their specific signaling needs (Licht and Jantsch 2016). This is especially interesting in the context of disease states in which RNA editing levels are known to be altered, such as cancer (Paz-Yaacov et al. 2015; Pershina and Arkhipov 2016; Xiao et al. 2019; Zhang et al. 2019), amyotrophic lateral sclerosis (ALS [Hideyama et al. 2012]), spinal cord injury (Di Narzo et al. 2015), Alzheimer's disease (Khermesh et al. 2016), arthritis (Vlachogiannis et al. 2019), hypoxia (Nevo-Caspi et al. 2011), and rheumatoid arthritis (Vlachogiannis et al. 2019).

In summary, A-to-I editing of $mGlu_4$ transcripts predicts the nonsynonymous substitution of two amino acids within the dimer interface of the resulting receptor, increasing proteome diversity. The RNA secondary structure necessary for editing presumably evolved in a common ancestor of mammals and is well conserved. The amino acid substitutions induced by RNA editing did not cause any gross alterations in receptor function in response to various endogenous and synthetic agonists, or allosteric modulators. Furthermore, Q124R substitution by RNA editing was demonstrated to alter the propensity of $mGlu_4$ to heterodimerize with the group II and III mGlu receptors, $mGlu_2$ and $mGlu_7$, respectively.

MATERIALS AND METHODS

Tissue collection

Rat tissue was collected from three untreated, 3–5-wk-old Sprague Dawley rats. Following euthanasia, brain regions were dissected, flash frozen in $N_{2\ (l)}$, and stored at −80°C until further processing. Samples were homogenized in 1 mL of TRIzol reagent (Invitrogen) by sonication (Sonic Dismembrator 100, Fisher Scientific) and processed according to the manufacturer's instructions. Human control RNA from tissues obtained from the NICHD Brain and Tissue Bank for Developmental Disorders (University of Maryland in Baltimore, MD) were processed for use in a previous

study and were comprised of five male (aged 45–57) and three female subjects (aged 33–43) (O'Neil et al. 2017).

High-throughput sequencing

RNA samples were analyzed for quantity and quality by NanoDrop (Thermo Fisher). cDNA was generated by random hexanucleotide primer, single strand synthesis using the High Capacity cDNA Reverse Transcriptase Kit (Applied Biosystems). Editing profiles were determined by high-throughput multiplexed transcript analysis (HTMTA) as described previously (Morabito et al. 2010a,b; O'Neil et al. 2017).

Bioinformatics

The RNA sequencing reads were composed of multiplexed samples, identifiable via a series of 6-nt barcodes. Instead of traditional short-read aligners to probe the sequence data, we used SeqKit (Shen et al. 2016), which supports regular expression-based fuzzy matching for identifying variants within otherwise fixed sequences in the short-read data. Within our workflow, we first demultiplexed the FastQ reads into their respective sample bins, and then performed an exact alignment of each barcoded read for the gene reference sequence out to 20-nt past the known RNA editing variant position, and at the same time allowed for variant nucleotides at the known position via fuzzy matching. Reads that did not exactly match the adapter sequence were discarded. The nucleotide frequency at each adenosine residue within the reference sequence was measured and used to determine an overall error rate for the polymerase of 0.243%. An adenosine at the corresponding position in the reference sequence was considered "not edited" while a guanosine above the error rate cutoff was considered "edited."

mfold

Sequences encoding either the human $mGlu_4$ or rat $mGlu_{4,\ 7}$, and $_8$ pre-mRNA were input into the *mfold* RNA folding form (http ://unafold.rna.albany.edu/?q=mfold/RNA-Folding-Form) (Zuker 2003) and set to default constraints. An initial input of 9,000bp flanking the human Q124R edit site was used to determine an initial putative fold. Rat $mGlu_{4,\ 7}$, and $_8$ sequences were then constrained to sequence homologous to this initial putative duplex and folded under default folding constraints. Mutations introduced into $mGlu_4$ minigenes were evaluated in *mfold* to predict destabilization or restabilization of the duplex.

ClustalW/Tcoffee

$mGlu_4$ transcripts from multiple species [Alligator (XM_00602 5093.3), Sea Turtle (XM_0278259655.1), Amoenefish (XM_0232 75611.1), Crow (XM_088644711.2), Chicken (XM_015298989.2), Human (NM_000841.4), Glassy Fish (XM_028409706.1), Macaque (XM_0015136121.1), Mouse (XM_001291045.1), Chimpanzee (XM_0094510151.3), Rat (NM_022666.1), Eel (XM_026 333481.1), Sparrow (XM_005492784.3), Human mlu7 (NM_008 44.4), Human mGlu8 (NM_00845.2), Rat mGlu7 (NM_031040.1), Rat mGlu8 (NM_022202.1), Rat mGlu6 (NM_022920.1)] were collected from the National Center for Biotechnology Information (NCBI). Alignments were conducted using T-COFFEE (Version 11.00.d625267) set to default settings. Output Clustalw alignment files were visualized and % identity to the human sequence was determined using JalView (Waterhouse et al. 2009).

Structural modeling

Homology models of $mGlu_4$ extracellular domains were generated using x-ray crystal structures of $mGlu_5$ in either an apo (inactive) state (PDB: 6N4X) or agonist-bound (active) state (PDB: 6N50) (Koehl et al. 2019). The $mGlu_4$ sequence was threaded onto both templates before the global model was optimized using the ICMpro software package (Molsoft) as described in PDBID: 8710833, 9485492. The structure of any loop regions that were absent from the template models were predicted using local energy optimization as described in PDBID: 11045621. The final resultant models were visually inspected to ensure they were consistent with published biological data. To examine the influence of the RNA editing of the Q124R to the $mGlu_4$ dimer interface, the residue change was sequentially introduced into the apo and agonist-bound models, which were then sampled independently. Sampling involved randomization of sidechain residues within Helix B and the adjacent loop of each protomer using Monte Carlo randomization and energy scoring (model sampled 5 e^5 times per randomization), followed by whole-model energy minimization. Multiple poses were retained from sampling where the overall RMSD of Q/R124 side chain atoms after energy minimization varied by more than 0.1 Å. The process yielded six homology models for $mGlu_4$: inactive Q124/Q124, inactive Q124/R124, inactive R124/R124, active Q124/Q124, active Q124/R124, active R124/R124. Visual inspection, analysis and images for publication of final models was performed using PyMOL (Schrödinger Inc).

Plasmid constructs

Construction of the rat FLAG-ADAR2b construct has been described previously (Singh et al. 2007). Mouse ADAR p110 was cloned into pCMV Sport (Addgene) at Sal1/Not1 sites. pIRES constructs encoding $mGlu_4$, $mGlu_7$, or $mGlu_8$ served as a template to generate additional mGlu constructs. MYC-$mGlu_4$ was generated using a synthetic oligonucleotide designed to insert the MYC epitope tag into the amino-terminal BstEII site of $mGlu_4$ after the signal peptide as in Han and Hampson (1999) and cloned into pcDNA3 at BamHI/Not1 sites. $mGlu_4$, C1 and C2 constructs were generated by the introduction of a Not1 site by Site Directed Mutagenesis (Qiagen Quikchange II XL) between (T874–Q875). The carboxy-terminal tail of the receptor was removed by Not1 digest, after which gBlock Gene Fragments (IDT) encoding either the C1 or C2 terminal tail of the $GABA_B$ receptor followed by the ER retention signal KTTN (Huang et al. 2011) were subcloned into the Not1 site. All single nucleotide changes for edited constructs were made by site directed mutagenesis (Qiagen Quikchange II XL) according to the manufacturer's instructions. The carboxy-terminally tagged ELNF1-Myc construct (Dunn et al. 2018) was constructed by amplifying from mouse ELFN1 cDNA clone (Clone ID 6811341, Open Biosystems) and subcloning into pcDNA3 at the BamHI/EcoRI

sites. All $mGlu_4$ minigenes were purchased as gBlocks and subcloned into pcDNA3 at BamHI/EcoRI sites.

Cell culture

All cells were maintained in a 37°C incubator with 5% CO_2. HEK293-GIRK parental cells were passaged in media (50% DMEM, 50% F12, supplemented with 10% FBS, 20 mM HEPES, 1 mM Na Pyruvate, 2 mM Glutamax, 0.1 mM nonessential amino acids, 1× antibiotic/antimycotic) under G418 (700 µg/mL) selection to maintain GIRK expression. HEK293-GIRK cells stably expressing rat $mGlu_4$ constructs were additionally maintained under puromycin (600 ng/mL) selection. HEK293A polyclonal cells stably expressing either ELFN1 or empty vector were passaged in media (DMEM, supplemented with 10% FBS, 20 mM HEPES, 1 mM Na Pyruvate, 2 mM Glutamax, 0.1 mM nonessential amino acids, 1× antibiotic/antimycotic) under G418 (700 µg/mL) selection to maintain expression. Cells were transfected using Fugene6 transfection reagent (Promega) according to the manufacturer's protocol.

In vitro editing assay

HEK293T cells plated in 6 well culture dishes were transfected with either an $mGlu_4$ minigene construct alone, or cotransfected with ADAR1 P110 or FLAG-ADAR2b. Forty-eight hours post transfection, cells were rinsed with HBSS and lysed in 1 mL of TRIzol. RNA was extracted according to the manufacturer's instructions and DNased using Turbo DNAfree (Life Technologies). To further limit genomic contamination, cDNA was made using the High Capacity cDNA Kit according to the manufacturer's protocol, except an $mGlu_4$ specific primer with a unique sequence overhang was substituted in place of the random hexanucleotide primers. Primers complementary to $mGlu_4$ and the unique nucleotide sequence were used to amplify $mGlu_4$ minigenes for Sanger sequencing. Percentage editing was determined by analysis of chromatogram peak heights in ImageJ. Samples with no discernable "A" or "G" peak were given a value of "0."

Thallium flux assays

Cells were plated in black walled, clear bottomed, amine-coated 384 well plates (Ref#356719, Corning) at 15,000 cells/20 µL/well in assay media (DMEM, supplemented with 10% dialyzed FBS, 20 mM HEPES, 1 mM Na Pyruvate, 1× antibiotic/antimycotic) devoid of exogenous glutamate. For experiments involving ELFN1, stable cell lines were mixed to a ratio of 2:1 ELFN1- or vector-expressing cells: $mGlu_4$-expressing cells before plating. Assay dye loading, compound addition, and experimental measurement procedures have been described previously (Yin et al. 2014). This assay was developed in our laboratory and first described in Niswender et al. (2008). In short, glutamate stimulates the activation of $G_{i/o}$ heterotrimeric G-proteins via transfected mGlu receptors. Dissociated Bγ subunits then directly stimulate the opening of GIRK channels, increasing the rate of influx of extracellularly applied thallium and leading to activation of an intracellular dye, Fluozin-2AM. HEK293 cells stably expressing GIRK channels demonstrate a background level of thallium flux; however, that flux is not modulated in response to glutamate. Basal flux, defined by the kinetic rate of thallium entry in cells into the absence of glutamate, is subtracted from all values to obtain the agonist-induced signal. Signal obtained from different experimental days is normalized to the % response of a control protein, in this case, the nonedited receptor condition. % response is calculated by expressing fluorescent values as a percentage of the maximal fluorescent response obtained to glutamate at saturation for a particular control condition.

Western blot

On day 1 following transfection, media of transfected cells was replaced with Opti-MEM (Gibco, 11058-021) containing 2% added FBS serum. On Day 2, media was collected and centrifuged at 500*g* to remove floating cells and debris. The media supernatant was collected and concentrated to ~250 µL using an Amicon Ultracel-50K (Millipore, UFC805024) according to the manufacturer instructions. Cells were rinsed and lifted by scraping in ice-cold PBS and collected by centrifugation at 500*g*. Cells pellets were lysed in RIPA buffer (Sigma, R0278) with 1× Complete Protease Inhibitor (Roche, 04693124001) on ice for 30 min. Supernatant was separated from insoluble cell debris by centrifugation at 20,000*g* for 20 min. Protein concentration was assessed by BCA (Thermo Scientific, 23225). Proteins were separated by SDS-PAGE (Bio-Rad, 465-1095) and transferred to a nitrocellulose membrane using the iBlot2 transfer system (Thermo Fisher) at 20 volts for 8 min. Membranes were blocked using Intercept TBS blocking buffer (LiCor, 927-60001) and incubated with rabbit anti-Myc (Cell Signaling, 71D10) diluted 1:1000 in blocking buffer overnight at 4°C. Membranes were washed in TBST (Sigma, T5912) and incubated for 1 h at room temperature with goat anti-rabbit 800CW (LiCor, 926-3211) diluted 1:5000 in blocking buffer. Membranes were again washed with TBST and imaged using a Licor Odyssey scanner. Membranes were then reblocked for 30 min and incubated with mouse anti-GAPDH (Thermo Fisher, MA-5-15738) for 1 h at room temperature. Following washing with TBST, membranes were incubated with 1:10,000 diluted goat anti-mouse 680LT (LiCor, 926-68020), washed with TBST, and imaged using a LiCor Odyssey scanner. Analysis was conducted using Image Studio Lite (LiCor). Fluorescent values for Myc signal were normalized to those of GAPDH.

Dimerization assay

Black walled, clear bottom 96 well plates (Corning, #3764) were coated with Poly-D-Lysine hydrobromide solution (Sigma, P64075 mg) for 24 h prior to cell plating according to the manufacturer's protocol. HEK293-GIRK parental cells transiently transfected with a 2:1 µg ratio of plasmid encoding the truncated, secretable MYC-tagged $mGlu_4$ to HA-tagged full length mGlu construct were plated at 100,000 cells/well in assay media. The following day, cells were washed in PBS, fixed in 4% paraformaldehyde (in PBS, pH 7.4) for 20 min at room temperature, and washed 4 × 5 min in PBS. After blocking for 1.5 h in Intercept (PBS) Blocking Buffer (LiCor), cells were stained with either 1:1000 Rabbit anti-HA (Abcam, Ab9110) or 1:1000 Mouse Anti-MYC (Cell Signaling, 9B11 mAB) and 1:1000 DRAQ5 (Thermo Fisher) overnight at 4°C with rocking. Cells were washed

5 × 5 min in PBS-T (0.01%Tween-20), stained with 1:15,000 IR Dye 800CW Donkey anti Mouse (LiCor) or 1:15,000 IR Dye 800CW Donkey anti Rabbit (LiCor). Fluorescent labeling of Myc and HA tags was determined in separate wells due to overlap in spectra of the secondary antibodies used for detection. Within each well, fluorescent values for MYC or HA signal were normalized to that of the DRAQ5 nuclear stain. Three to six technical replicates' of normalized values were averaged for each condition and the average normalized HA or Myc signal of untransfected control cells was subtracted as a blank from all values. Propensity to dimerize was determined by dividing the Myc signal of the secretable $mGlu_4$ ATD by that of the HA signal for the full length, cotransfected mGlu receptor. Data were normalized across days by normalizing all conditions to that of the response of nonedited $mGlu_4$.

ACKNOWLEDGMENTS

We are grateful for the support of Dr. Jean-Philippe Cartailler of the Vanderbilt Creative Data Solutions Shared Resource, who developed the workflow for identifying RNA-editing events in short-read HTS data and tabulated the results.

Received March 1, 2021; accepted July 1, 2021.

REFERENCES

Antflick JE, Hampson DR. 2012. Modulation of glutamate release from parallel fibers by mGlu4 and pre-synaptic $GABA_A$ receptors. *J Neurochem* **120:** 552–563. doi:10.1111/j.1471-4159.2011.07611.x

Bass BL. 2002. RNA editing by adenosine deaminases that act on RNA. *Annu Rev Biochem* **71:** 817–846. doi:10.1146/annurev.biochem.71.110601.135501

Bhalla T, Rosenthal JJ, Holmgren M, Reenan R. 2004. Control of human potassium channel inactivation by editing of a small mRNA hairpin. *Nat Struct Mol Biol* **11:** 950–956. doi:10.1038/nsmb825

Blednov YA, Walker D, Osterndorf-Kahanek E, Harris RA. 2004. Mice lacking metabotropic glutamate receptor 4 do not show the motor stimulatory effect of ethanol. *Alcohol* **34:** 251–259. doi:10.1016/j.alcohol.2004.10.003

Bradley SR, Standaert DG, Levey AI, Conn PJ. 1999. Distribution of group III mGluRs in rat basal ganglia with subtype-specific antibodies. *Ann N Y Acad Sci* **868:** 531–534. doi:10.1111/j.1749-6632.1999.tb11322.x

Brice NL, Varadi A, Ashcroft SJ, Molnar E. 2002. Metabotropic glutamate and $GABA_B$ receptors contribute to the modulation of glucose-stimulated insulin secretion in pancreatic β cells. *Diabetologia* **45:** 242–252. doi:10.1007/s00125-001-0750-0

Burns CM, Chu H, Rueter SM, Hutchinson LK, Canton H, Sanders-Bush E, Emeson RB. 1997. Regulation of serotonin-2C receptor G-protein coupling by RNA editing. *Nature* **387:** 303–308. doi:10.1038/387303a0

Carmel L, Koonin EV, Dracheva S. 2012. Dependencies among editing sites in serotonin 2C receptor mRNA. *PLoS Comput Biol* **8:** e1002663. doi:10.1371/journal.pcbi.1002663

Chalk AM, Taylor S, Heraud-Farlow JE, Walkley CR. 2019. The majority of A-to-I RNA editing is not required for mammalian homeostasis. *Genome Biol* **20:** 268. doi:10.1186/s13059-019-1873-2

Chang HJ, Yoo BC, Lim SB, Jeong SY, Kim WH, Park JG. 2005. Metabotropic glutamate receptor 4 expression in colorectal carcinoma and its prognostic significance. *Clin Cancer Res* **11:** 3288–3295. doi:10.1158/1078-0432.CCR-04-1912

Chardonnet S, Bessiron T, Ramos CI, Dammak R, Richard MA, Boursier C, Cadilhac C, Coquelle FM, Bossi S, Ango F, et al. 2017. Native metabotropic glutamate receptor 4 depresses synaptic transmission through an unusual $G\alpha_q$ transduction pathway. *Neuropharmacology* **121:** 247–260. doi:10.1016/j.neuropharm.2017.04.036

Costa Cruz PH, Kato Y, Nakahama T, Shibuya T, Kawahara Y. 2020. A comparative analysis of ADAR mutant mice reveals site-specific regulation of RNA editing. *RNA* **26:** 454–469. doi:10.1261/rna.072728.119

Desterro JM, Keegan LP, Lafarga M, Berciano MT, O'Connell M, Carmo-Fonseca M. 2003. Dynamic association of RNA-editing enzymes with the nucleolus. *J Cell Sci* **116:** 1805–1818. doi:10.1242/jcs.00371

Di Narzo AF, Kozlenkov A, Ge Y, Zhang B, Sanelli L, May Z, Li Y, Fouad K, Cardozo C, Koonin EV, et al. 2015. Decrease of mRNA editing after spinal cord injury is caused by down-regulation of ADAR2 that is triggered by inflammatory response. *Sci Rep* **5:** 12615. doi:10.1038/srep12615

Doumazane E, Scholler P, Zwier JM, Trinquet E, Rondard P, Pin JP. 2011. A new approach to analyze cell surface protein complexes reveals specific heterodimeric metabotropic glutamate receptors. *FASEB J* **25:** 66–77. doi:10.1096/fj.10-163147

Dunn HA, Patil DN, Cao Y, Orlandi C, Martemyanov KA. 2018. Synaptic adhesion protein ELFN1 is a selective allosteric modulator of group III metabotropic glutamate receptors in *trans*. *Proc Natl Acad Sci* **115:** 5022–5027. doi:10.1073/pnas.1722498115

Eggington JM, Greene T, Bass BL. 2011. Predicting sites of ADAR editing in double-stranded RNA. *Nat Commun* **2:** 319. doi:10.1038/ncomms1324

El Moustaine D, Granier S, Doumazane E, Scholler P, Rahmeh R, Bron P, Mouillac B, Baneres JL, Rondard P, Pin JP. 2012. Distinct roles of metabotropic glutamate receptor dimerization in agonist activation and G-protein coupling. *Proc Natl Acad Sci* **109:** 16342–16347. doi:10.1073/pnas.1205838109

Fallarino F, Volpi C, Fazio F, Notartomaso S, Vacca C, Busceti C, Bicciato S, Battaglia G, Bruno V, Puccetti P, et al. 2010. Metabotropic glutamate receptor-4 modulates adaptive immunity and restrains neuroinflammation. *Nat Med* **16:** 897–902. doi:10.1038/nm.2183

Flor PJ, Lukic S, Ruegg D, Leonhardt T, Knopfel T, Kuhn R. 1995. Molecular cloning, functional expression and pharmacological characterization of the human metabotropic glutamate receptor type 4. *Neuropharmacology* **34:** 149–155. doi:10.1016/0028-3908(94)00149-M

Forni D, Mozzi A, Pontremoli C, Vertemara J, Pozzoli U, Biasin M, Bresolin N, Clerici M, Cagliani R, Sironi M. 2015. Diverse selective regimes shape genetic diversity at ADAR genes and at their coding targets. *RNA Biol* **12:** 149–161. doi:10.1080/15476286.2015.1017215

Habrian CH, Levitz J, Vyklicky V, Fu Z, Hoagland A, McCort-Tranchepain I, Acher F, Isacoff EY. 2019. Conformational pathway provides unique sensitivity to a synaptic mGluR. *Nat Commun* **10:** 5572. doi:10.1038/s41467-019-13407-8

Han G, Hampson DR. 1999. Ligand binding to the amino-terminal domain of the mGluR4 subtype of metabotropic glutamate receptor. *J Biol Chem* **274:** 10008–10013. doi:10.1074/jbc.274.15.10008

Herb A, Higuchi M, Sprengel R, Seeburg PH. 1996. Q/R site editing in kainate receptor GluR5 and GluR6 pre-mRNAs requires distant intronic sequences. *Proc Natl Acad Sci* **93:** 1875–1880. doi:10.1073/pnas.93.5.1875

Hideyama T, Yamashita T, Aizawa H, Tsuji S, Kakita A, Takahashi H, Kwak S. 2012. Profound downregulation of the RNA editing enzyme ADAR2 in ALS spinal motor neurons. *Neurobiol Dis* **45:** 1121–1128. doi:10.1016/j.nbd.2011.12.033

Hoopengardner B, Bhalla T, Staber C, Reenan R. 2003. Nervous system targets of RNA editing identified by comparative genomics. *Science* **301:** 832–836. doi:10.1126/science.1086763

Huang S, Cao J, Jiang M, Labesse G, Liu J, Pin JP, Rondard P. 2011. Interdomain movements in metabotropic glutamate receptor activation. *Proc Natl Acad Sci* **108:** 15480–15485. doi:10.1073/pnas.1107775108

Iacovelli L, Bruno V, Salvatore L, Melchiorri D, Gradini R, Caricasole A, Barletta E, De Blasi A, Nicoletti F. 2002. Native group-III metabotropic glutamate receptors are coupled to the mitogen-activated protein kinase/phosphatidylinositol-3-kinase pathways. *J Neurochem* **82:** 216–223. doi:10.1046/j.1471-4159.2002.00929.x

Iacovelli L, Arcella A, Battaglia G, Pazzaglia S, Aronica E, Spinsanti P, Caruso A, De Smaele E, Saran A, Gulino A, et al. 2006. Pharmacological activation of mGlu4 metabotropic glutamate receptors inhibits the growth of medulloblastomas. *J Neurosci* **26:** 8388–8397. doi:10.1523/JNEUROSCI.2285-06.2006

Jain M, Mann TD, Stulic M, Rao SP, Kirsch A, Pullirsch D, Strobl X, Rath C, Reissig L, Moreth K, et al. 2018. RNA editing of Filamin A pre-mRNA regulates vascular contraction and diastolic blood pressure. *EMBO J* **37:** e94813. doi:10.15252/embj.201694813

Jinnah H, Ulbricht RJ. 2019. Using mouse models to unlock the secrets of non-synonymous RNA editing. *Methods* **156:** 40–45. doi:10.1016/j.ymeth.2018.10.016

Julio-Pieper M, Flor PJ, Dinan TG, Cryan JF. 2011. Exciting times beyond the brain: metabotropic glutamate receptors in peripheral and non-neural tissues. *Pharmacol Rev* **63:** 35–58. doi:10.1124/pr.110.004036

Kammermeier PJ. 2012. Functional and pharmacological characteristics of metabotropic glutamate receptors 2/4 heterodimers. *Mol Pharmacol* **82:** 438–447. doi:10.1124/mol.112.078501

Khermesh K, D'Erchia AM, Barak M, Annese A, Wachtel C, Levanon EY, Picardi E, Eisenberg E. 2016. Reduced levels of protein recoding by A-to-I RNA editing in Alzheimer's disease. *RNA* **22:** 290–302. doi:10.1261/rna.054627.115

Kishimoto M, Hashiramoto M, Yonezawa K, Shii K, Kazumi T, Kasuga M. 1994. Substitution of glutamine for arginine 1131. A newly identified mutation in the catalytic loop of the tyrosine kinase domain of the human insulin receptor. *J Biol Chem* **269:** 11349–11355. doi:10.1016/S0021-9258(19)78131-9

Koehl A, Hu H, Feng D, Sun B, Zhang Y, Robertson MJ, Chu M, Kobilka TS, Laeremans T, Steyaert J, et al. 2019. Structural insights into the activation of metabotropic glutamate receptors. *Nature* **566:** 79–84. doi:10.1038/s41586-019-0881-4

Kosinski CM, Risso Bradley S, Conn PJ, Levey AI, Landwehrmeyer GB, Penney JB Jr, Young AB, Standaert DG. 1999. Localization of metabotropic glutamate receptor 7 mRNA and mGluR7a protein in the rat basal ganglia. *J Comp Neurol* **415:** 266–284. doi:10.1002/(SICI)1096-9861(19991213)415:2<266::AID-CNE9>3.0.CO;2-7

Kunishima N, Shimada Y, Tsuji Y, Sato T, Yamamoto M, Kumasaka T, Nakanishi S, Jingami H, Morikawa K. 2000. Structural basis of glutamate recognition by a dimeric metabotropic glutamate receptor. *Nature* **407:** 971–977. doi:10.1038/35039564

Lebourgeois S, Vilpoux C, Jeanblanc J, Acher F, Marie N, Noble F, Naassila M. 2018. Pharmacological activation of mGlu4 and mGlu7 receptors, by LSP2-9166, reduces ethanol consumption and relapse in rat. *Neuropharmacology* **133:** 163–170. doi:10.1016/j.neuropharm.2018.01.031

Lee J, Munguba H, Gutzeit VA, Kristt M, Dittman JS, Levitz J. 2020. Defining the homo- and heterodimerization propensities of metabotropic glutamate receptors. *Cell Rep* **31:** 107605. doi:10.1016/j.celrep.2020.107605

Levanon EY, Eisenberg E, Yelin R, Nemzer S, Hallegger M, Shemesh R, Fligelman ZY, Shoshan A, Pollock SR, Sztybel D, et al. 2004. Systematic identification of abundant A-to-I editing sites in the human transcriptome. *Nat Biotechnol* **22:** 1001–1005. doi:10.1038/nbt996

Levitz J, Habrian C, Bharill S, Fu Z, Vafabakhsh R, Isacoff EY. 2016. Mechanism of assembly and cooperativity of homomeric and heteromeric metabotropic glutamate receptors. *Neuron* **92:** 143–159. doi:10.1016/j.neuron.2016.08.036

Li JB, Levanon EY, Yoon JK, Aach J, Xie B, Leproust E, Zhang K, Gao Y, Church GM. 2009. Genome-wide identification of human RNA editing sites by parallel DNA capturing and sequencing. *Science* **324:** 1210–1213. doi:10.1126/science.1170995

Licht K, Jantsch MF. 2016. Rapid and dynamic transcriptome regulation by RNA editing and RNA modifications. *J Cell Biol* **213:** 15–22. doi:10.1083/jcb.201511041

Licht K, Kapoor U, Mayrhofer E, Jantsch MF. 2016. Adenosine to Inosine editing frequency controlled by splicing efficiency. *Nucleic Acids Res* **44:** 6398–6408. doi:10.1093/nar/gkw325

Licht K, Kapoor U, Amman F, Picardi E, Martin D, Bajad P, Jantsch MF. 2019. A high resolution A-to-I editing map in the mouse identifies editing events controlled by pre-mRNA splicing. *Genome Res* **29:** 1453–1463. doi:10.1101/gr.242636.118

Lorez M, Humbel U, Pflimlin MC, Kew JN. 2003. Group III metabotropic glutamate receptors as autoreceptors in the cerebellar cortex. *Br J Pharmacol* **138:** 614–625. doi:10.1038/sj.bjp.0705099

Makoff A, Lelchuk R, Oxer M, Harrington K, Emson P. 1996. Molecular characterization and localization of human metabotropic glutamate receptor type 4. *Brain Res Mol Brain Res* **37:** 239–248. doi:10.1016/0169-328X(95)00321-I

Melcher T, Maas S, Herb A, Sprengel R, Higuchi M, Seeburg PH. 1996a. RED2, a brain-specific member of the RNA-specific adenosine deaminase family. *J Biol Chem* **271:** 31795–31798. doi:10.1074/jbc.271.50.31795

Melcher T, Maas S, Herb A, Sprengel R, Seeburg PH, Higuchi M. 1996b. A mammalian RNA editing enzyme. *Nature* **379:** 460–464. doi:10.1038/379460a0

Meldrum BS. 2000. Glutamate as a neurotransmitter in the brain: review of physiology and pathology. *J Nutr* **130:** 1007S–1015S. doi:10.1093/jn/130.4.1007S

Miyake K, Ohta T, Nakayama H, Doe N, Terao Y, Oiki E, Nagatomo I, Yamashita Y, Abe T, Nishikura K, et al. 2016. CAPS1 RNA editing promotes dense core vesicle exocytosis. *Cell Rep* **17:** 2004–2014. doi:10.1016/j.celrep.2016.10.073

Morabito MV, Abbas AI, Hood JL, Kesterson RA, Jacobs MM, Kump DS, Hachey DL, Roth BL, Emeson RB. 2010a. Mice with altered serotonin 2C receptor RNA editing display characteristics of Prader-Willi syndrome. *Neurobiol Dis* **39:** 169–180. doi:10.1016/j.nbd.2010.04.004

Morabito MV, Ulbricht RJ, O'Neil RT, Airey DC, Lu P, Zhang B, Wang L, Emeson RB. 2010b. High-throughput multiplexed transcript analysis yields enhanced resolution of 5-hydroxytryptamine 2C receptor mRNA editing profiles. *Mol Pharmacol* **77:** 895–902. doi:10.1124/mol.109.061903

Moreno Delgado D, Moller TC, Ster J, Giraldo J, Maurel D, Rovira X, Scholler P, Zwier JM, Perroy J, Durroux T, et al. 2017. Pharmacological evidence for a metabotropic glutamate receptor heterodimer in neuronal cells. *Elife* **6:** e25233. doi:10.7554/eLife.25233

Muto T, Tsuchiya D, Morikawa K, Jingami H. 2007. Structures of the extracellular regions of the group II/III metabotropic glutamate receptors. *Proc Natl Acad Sci* **104:** 3759–3764. doi:10.1073/pnas.0611577104

Nevo-Caspi Y, Amariglio N, Rechavi G, Paret G. 2011. A-to-I RNA editing is induced upon hypoxia. *Shock* **35:** 585–589. doi:10.1097/SHK.0b013e31820fe4b7

Niswender CM, Conn PJ. 2010. Metabotropic glutamate receptors: physiology, pharmacology, and disease. *Annu Rev Pharmacol Toxicol* **50:** 295–322. doi:10.1146/annurev.pharmtox.011008.145533

Niswender CM, Johnson KA, Luo Q, Ayala JE, Kim C, Conn PJ, Weaver CD. 2008. A novel assay of $G_{i/o}$-linked G protein-coupled receptor coupling to potassium channels provides new insights into the pharmacology of the group III metabotropic glutamate receptors. *Mol Pharmacol* **73:** 1213–1224. doi:10.1124/mol.107.041053

Niswender CM, Jones CK, Lin X, Bubser M, Thompson Gray A, Blobaum AL, Engers DW, Rodriguez AL, Loch MT, Daniels JS, et al. 2016. Development and antiparkinsonian activity of VU0418506, a selective positive allosteric modulator of metabotropic glutamate receptor 4 homomers without activity at $mGlu_{2/4}$ heteromers. *ACS Chem Neurosci* **7:** 1201–1211. doi:10.1021/acschemneuro.6b00036

Ohlson J, Pedersen JS, Haussler D, Ohman M. 2007. Editing modifies the $GABA_A$ receptor subunit α3. *RNA* **13:** 698–703. doi:10.1261/rna.349107

O'Neil RT, Wang X, Morabito MV, Emeson RB. 2017. Comparative analysis of A-to-I editing in human and non-human primate brains reveals conserved patterns and context-dependent regulation of RNA editing. *Mol Brain* **10:** 11. doi:10.1186/s13041-017-0291-1

Patterson JB, Samuel CE. 1995. Expression and regulation by interferon of a double-stranded-RNA-specific adenosine deaminase from human cells: evidence for two forms of the deaminase. *Mol Cell Biol* **15:** 5376–5388. doi:10.1128/MCB.15.10.5376

Paz-Yaacov N, Bazak L, Buchumenski I, Porath HT, Danan-Gotthold M, Knisbacher BA, Eisenberg E, Levanon EY. 2015. Elevated RNA editing activity is a major contributor to transcriptomic diversity in tumors. *Cell Rep* **13:** 267–276. doi:10.1016/j.celrep.2015.08.080

Pershina EV, Arkhipov VI. 2016. Subacute activation of mGlu4 receptors causes the feedback inhibition of its gene expression in rat brain. *Life Sci* **153:** 50–54. doi:10.1016/j.lfs.2016.03.033

Pestal K, Funk CC, Snyder JM, Price ND, Treuting PM, Stetson DB. 2015. Isoforms of RNA-editing enzyme ADAR1 independently control nucleic acid sensor MDA5-driven autoimmunity and multi-organ development. *Immunity* **43:** 933–944. doi:10.1016/j.immuni.2015.11.001

Pinto Y, Cohen HY, Levanon EY. 2014. Mammalian conserved ADAR targets comprise only a small fragment of the human editosome. *Genome Biol* **15:** R5. doi:10.1186/gb-2014-15-1-r5

Polson AG, Bass BL. 1994. Preferential selection of adenosines for modification by double-stranded RNA adenosine deaminase. *EMBO J* **13:** 5701–5711. doi:10.1002/j.1460-2075.1994.tb06908.x

Ponnazhagan R, Harms AS, Thome AD, Jurkuvenaite A, Gogliotti R, Niswender CM, Conn PJ, Standaert DG. 2016. The metabotropic glutamate receptor 4 positive allosteric modulator ADX88178 inhibits inflammatory responses in primary microglia. *J Neuroimmune Pharmacol* **11:** 231–237. doi:10.1007/s11481-016-9655-z

Poulsen H, Nilsson J, Damgaard CK, Egebjerg J, Kjems J. 2001. CRM1 mediates the export of ADAR1 through a nuclear export signal within the Z-DNA binding domain. *Mol Cell Biol* **21:** 7862–7871. doi:10.1128/MCB.21.22.7862-7871.2001

Prudente S, Hribal ML, Flex E, Turchi F, Morini E, De Cosmo S, Bacci S, Tassi V, Cardellini M, Lauro R, et al. 2005. The functional Q84R polymorphism of mammalian *Tribbles* homolog *TRB3* is associated with insulin resistance and related cardiovascular risk in Caucasians from Italy. *Diabetes* **54:** 2807–2811. doi:10.2337/diabetes.54.9.2807

Ramaswami G, Zhang R, Piskol R, Keegan LP, Deng P, O'Connell MA, Li JB. 2013. Identifying RNA editing sites using RNA sequencing data alone. *Nat Methods* **10:** 128–132. doi:10.1038/nmeth.2330

Reenan RA. 2005. Molecular determinants and guided evolution of species-specific RNA editing. *Nature* **434:** 409–413. doi:10.1038/nature03364

Reiner A, Levitz J. 2018. Glutamatergic signaling in the central nervous system: ionotropic and metabotropic receptors in concert. *Neuron* **98:** 1080–1098. doi:10.1016/j.neuron.2018.05.018

Robbins MJ, Ciruela F, Rhodes A, McIlhinney RA. 1999. Characterization of the dimerization of metabotropic glutamate receptors using an N-terminal truncation of mGluR1α. *J Neurochem* **72:** 2539–2547. doi:10.1046/j.1471-4159.1999.0722539.x

Rosenthal JJ, Seeburg PH. 2012. A-to-I RNA editing: effects on proteins key to neural excitability. *Neuron* **74:** 432–439. doi:10.1016/j.neuron.2012.04.010

Sansam CL, Wells KS, Emeson RB. 2003. Modulation of RNA editing by functional nucleolar sequestration of ADAR2. *Proc Natl Acad Sci* **100:** 14018–14023. doi:10.1073/pnas.2336131100

Sato T, Shimada Y, Nagasawa N, Nakanishi S, Jingami H. 2003. Amino acid mutagenesis of the ligand binding site and the dimer interface of the metabotropic glutamate receptor 1. Identification of crucial residues for setting the activated state. *J Biol Chem* **278:** 4314–4321. doi:10.1074/jbc.M210278200

Savva YA, Rieder LE, Reenan RA. 2012. The ADAR protein family. *Genome Biol* **13:** 252. doi:10.1186/gb-2012-13-12-252

Semyanov A, Kullmann DM. 2000. Modulation of GABAergic signaling among interneurons by metabotropic glutamate receptors. *Neuron* **25:** 663–672. doi:10.1016/S0896-6273(00)81068-5

Shen W, Le S, Li Y, Hu F. 2016. SeqKit: a cross-platform and ultrafast toolkit for FASTA/Q file manipulation. *PLoS One* **11:** e0163962. doi:10.1371/journal.pone.0163962

Singh M, Kesterson RA, Jacobs MM, Joers JM, Gore JC, Emeson RB. 2007. Hyperphagia-mediated obesity in transgenic mice misexpressing the RNA-editing enzyme ADAR2. *J Biol Chem* **282:** 22448–22459. doi:10.1074/jbc.M700265200

Sokalingam S, Raghunathan G, Soundrarajan N, Lee SG. 2012. A study on the effect of surface lysine to arginine mutagenesis on protein stability and structure using green fluorescent protein. *PLoS One* **7:** e40410. doi:10.1371/journal.pone.0040410

Tan MH, Li Q, Shanmugam R, Piskol R, Kohler J, Young AN, Liu KI, Zhang R, Ramaswami G, Ariyoshi K, et al. 2017. Dynamic landscape and regulation of RNA editing in mammals. *Nature* **550:** 249–254. doi:10.1038/nature24041

Tsuchiya D, Kunishima N, Kamiya N, Jingami H, Morikawa K. 2002. Structural views of the ligand-binding cores of a metabotropic glutamate receptor complexed with an antagonist and both glutamate and Gd^{3+}. *Proc Natl Acad Sci* **99:** 2660–2665. doi:10.1073/pnas.052708599

Uehara S, Muroyama A, Echigo N, Morimoto R, Otsuka M, Yatsushiro S, Moriyama Y. 2004. Metabotropic glutamate receptor type 4 is involved in autoinhibitory cascade for glucagon secretion by α-cells of islet of Langerhans. *Diabetes* **53:** 998–1006. doi:10.2337/diabetes.53.4.998

Vilar B, Busserolles J, Ling B, Laffray S, Ulmann L, Malhaire F, Chapuy E, Aissouni Y, Etienne M, Bourinet E, et al. 2013. Alleviating pain hypersensitivity through activation of type 4 metabotropic glutamate receptor. *J Neurosci* **33:** 18951–18965. doi:10.1523/JNEUROSCI.1221-13.2013

Vlachogiannis NI, Gatsiou A, Silvestris DA, Stamatelopoulos K, Tektonidou MG, Gallo A, Sfikakis PP, Stellos K. 2019. Increased adenosine-to-inosine RNA editing in rheumatoid arthritis. *J Autoimmun* **106:** 102329. doi:10.1016/j.jaut.2019.102329

Wahlstedt H, Daniel C, Enstero M, Ohman M. 2009. Large-scale mRNA sequencing determines global regulation of RNA editing during brain development. *Genome Res* **19:** 978–986. doi:10.1101/gr.089409.108

Wang Q, O'Brien PJ, Chen CX, Cho DS, Murray JM, Nishikura K. 2000. Altered G protein-coupling functions of RNA editing isoform and splicing variant serotonin$_{2C}$ receptors. *J Neurochem* **74:** 1290–1300. doi:10.1046/j.1471-4159.2000.741290.x

Waterhouse AM, Procter JB, Martin DM, Clamp M, Barton GJ. 2009. Jalview Version 2–a multiple sequence alignment editor and analysis workbench. *Bioinformatics* **25:** 1189–1191. doi:10.1093/bioinformatics/btp033

Willard SS, Koochekpour S. 2013. Glutamate, glutamate receptors, and downstream signaling pathways. *Int J Biol Sci* **9:** 948–959. doi:10.7150/ijbs.6426

Wong SK, Sato S, Lazinski DW. 2001. Substrate recognition by ADAR1 and ADAR2. *RNA* **7:** 846–858. doi:10.1017/S135583820101007X

Xiang Z, Lv X, Lin X, O'Brien DE, Altman MK, Lindsley CW, Javitch JA, Niswender CM, Conn PJ. 2021. Input-specific regulation of glutamatergic synaptic transmission in the medial prefrontal cortex by mGlu$_2$/mGlu$_4$ receptor heterodimers. *Sci Signal* **14:** eabd2319. doi:10.1126/scisignal.abd2319

Xiao B, Chen D, Zhou Q, Hang J, Zhang W, Kuang Z, Sun Z, Li L. 2019. Glutamate metabotropic receptor 4 (GRM4) inhibits cell proliferation, migration and invasion in breast cancer and is regulated by miR-328-3p and miR-370-3p. *BMC Cancer* **19:** 891. doi:10.1186/s12885-019-6068-4

Yablonovitch AL, Deng P, Jacobson D, Li JB. 2017. The evolution and adaptation of A-to-I RNA editing. *PLoS Genet* **13:** e1007064. doi:10.1371/journal.pgen.1007064

Yin S, Noetzel MJ, Johnson KA, Zamorano R, Jalan-Sakrikar N, Gregory KJ, Conn PJ, Niswender CM. 2014. Selective actions of novel allosteric modulators reveal functional heteromers of metabotropic glutamate receptors in the CNS. *J Neurosci* **34:** 79–94. doi:10.1523/JNEUROSCI.1129-13.2014

Zhang Z, Ma W, Wang L, Gong H, Tian Y, Zhang J, Liu J, Lu H, Chen X, Liu Y. 2015. Activation of type 4 metabotropic glutamate receptor attenuates oxidative stress-induced death of neural stem cells with inhibition of JNK and p38 MAPK signaling. *Stem Cells Dev* **24:** 2709–2722. doi:10.1089/scd.2015.0067

Zhang Z, Li N, Wei X, Chen B, Zhang Y, Zhao Y, Hu X, Hou S. 2019. GRM4 inhibits the proliferation, migration, and invasion of human osteosarcoma cells through interaction with CBX4. *Biosci Biotechnol Biochem* **84:** 279–289. doi:10.1080/09168451.2019.1673147

Zuker M. 2003. Mfold web server for nucleic acid folding and hybridization prediction. *Nucleic Acids Res* **31:** 3406–3415. doi:10.1093/nar/gkg595